Eastern Mediterranean surface water temperatures and d18O composition during deposition of sapropels in the late Quaternary

Emeis, K.C.; Schulz, H.; Struck, U.; Rossignol-Strick, M.; Erlenkeuser, H.; Howell, M.W.; Kroon, D.; Mackensen, A.; Ishizuka, S.; Oba, T.; Sakamoto, T.; Koizumi, I.

published in
Paleoceanography
2003

DOI (link to publisher)
10.1029/2000PA000617

document version
Publisher's PDF, also known as Version of record

Eastern Mediterranean surface water temperatures and $\delta^{18}O$ composition during deposition of sapropels in the late Quaternary

K.-C. Emeis,[1] H. Schulz,[1] U. Struck,[2] M. Rossignol-Strick,[3] H. Erlenkeuser,[4] M. W. Howell,[5] D. Kroon,[6] A. Mackensen,[7] S. Ishizuka,[8] T. Oba,[9] T. Sakamoto,[10] and I. Koizumi[10]

Received 4 December 2000; revised 19 March 2002; accepted 17 May 2002; published 11 February 2003.

[1] Water column stratification increased at climatic transitions from cold to warm periods during the late Quaternary and led to anoxic conditions and sapropel formation in the deep eastern Mediterranean basins. High-resolution data sets on sea-surface temperatures (SST) (estimated from $U^{k'}_{37}$ indices) and $\delta^{18}O$ of planktonic foraminifer calcite ($\delta^{18}O_{fc}$) across late Pleistocene sapropel intervals show that $\delta^{18}O_{fc}$ decreased (between 1 and 4.6‰) and SST increased (between 0.7° and 6.7°C). Maximal $\delta^{18}O_{seawater}$ depletion of eastern Mediterranean surface waters at the transition is between 0.5 and 3.0‰, and in all but one case exceeded the depletion seen in a western Mediterranean core. The depletion in $\delta^{18}O_{seawater}$ is most pronounced at sapropel bases, in agreement with an initial sudden input of monsoon-derived freshwater. Most sapropels coincide with warming trends of SST. The density decrease by initial freshwater input and continued warming of the sea surface pooled fresh water in the surface layer and prohibited deep convection down to ageing deep water emplaced during cold and arid glacial conditions. An exception to this pattern is "glacial" sapropel S6; its largest $\delta^{18}O_{seawater}$ depletion (3‰) is almost matched by the depletion in the western Mediterranean Sea, and it is accompanied by surface water cooling following an initially rapid warming phase. A second period of significant isotopic depletion is in isotope stage 6 at the 150 kyr insolation maximum. While not expressed as a sapropel due to cold SST, it is in accord with a strengthened monsoon in the southern catchment. *INDEX TERMS:* 1055 Geochemistry: Organic geochemistry; 1620 Global Change: Climate dynamics (3309); 4267 Oceanography: General: Paleoceanography; 9604 Information Related to Geologic Time: Cenozoic; *KEYWORDS:* Mediterranean Sea, sapropels, sea surface temperatures, oxygen isotopes, Quaternary

Citation: Emeis, K.-C., et al., Eastern Mediterranean surface water temperatures and $\delta^{18}O$ composition during deposition of sapropels in the late Quaternary, *Paleoceanography*, *18*(1), 1005, doi:10.1029/2000PA000617, 2003.

1. Introduction

[2] Sediment cores from the eastern basins of the Mediterranean Sea, and land sections of Neogene age in southern Italy, Sicily, and Crete contain series of sapropel layers (cm to m thick) sandwiched in hemipelagic, carbonate-rich and oxic sediments. The sapropels are rich in organic carbon, devoid of benthic organisms and often laminated, and were deposited during periods when the deep waters of the eastern basins were anoxic [*Emeis et al.*, 2000a; *Kidd et al.*, 1978; *Olausson*, 1961; *Passier et al.*, 1999]. Similar and in part isochronous organic-rich layers have been found in the western Mediterranean Sea [*Comas et al.*, 1996; *Cramp and O'Sullivan*, 1999; *Emeis et al.*, 1991], but their environment of formation is under debate [*Béthoux and Pierre*, 1999]. Deep water anoxia in the eastern Mediterranean Sea is linked to climate, as evidenced by the close correlation of sapropel intervals with maxima of insolation on the Northern Hemisphere (NH) and periods of decreasing ice volume (Figure 1a) [*Cita et al.*, 1977; *Hilgen*, 1991; *Lourens et al.*, 1996; *Rossignol-Strick*, 1983; *Vergnaud-Grazzini et al.*, 1977].

[3] Sapropel periods were preceded by and coincided with changes in surface and deep water conditions and in water mass circulation of the eastern basin. The modern Mediterranean Sea has an antiestuarine circulation system with three water masses: Surface water flows east across the Strait of Sicily to balance evaporation in the eastern basins.

[1]Baltic Sea Research Institute, Warnemuende, Germany.
[2]Institute of Paleontology and Historical Geology, University of Munich, Munich, Germany.
[3]Laboratoire de Paléobiologie et Palynologie, Université Pierre et Marie Curie, Paris, France.
[4]Leibniz-Laboratory for Radiometric Dating and Stable Isotope Research, Kiel University, Kiel, Germany.
[5]Department of Geological Sciences, University of South Carolina, Columbia, South Carolina, USA.
[6]Faculty of Earth Sciences, Vrije Universiteit Amsterdam, Amsterdam, Netherlands.
[7]Alfred-Wegener-Institut für Polar- und Meeresforschung, Bremerhaven, Germany.
[8]The Education Bureau of Aomori Prefecture, Seihoku Educational Office, Goshogawara, Japan.
[9]Graduate School of Environmental Earth Science, Hokkaido University, Sapporo, Japan.
[10]Department of Earth and Planetary Sciences, Graduate School of Science, Hokkaido University, Sapporo, Japan.

0883-8305/03/2000PA000617$12.00

Small seasonal differences in the density of surface waters result in the formation of the Eastern Mediterranean Deep Water (EMDW), as well as the Levantine Intermediate Water (LIW) [*Malanotte-Rizzolli and Bergamasco*, 1989]. Deep water forms today by winter convection in the Adriatic and the Aegean Seas when relatively fresh but cool water sinks and spreads out throughout the Ionian Sea and spills over the Mediterranean Ridge into the Levantine Basin [*Roether et al.*, 1996]. The residence time of this deep water is of order 80 years, short enough so that the oxygen saturation remains above 60% [*Krom*, 1995]. The modern LIW mass forms in the Rhodes Gyre, spreads out in a depth interval above 500 m and is cooled again in the Adriatic Sea [*Malanotte-Rizzolli and Bergamasco*, 1989]. It thus supplies a source of preconditioned dense water that cools and sinks as EMDW [*Wu and Haines*, 1996]. In some instances, the Rhodes Gyre region develops a vertically mixed convective chimney during winter cooling and produces Levantine Deep Water which admixes with EMDW.

[4] One prerequisite for stagnation of deep water during sapropel formation was a decrease in surface water density (relative to that of deep water masses) that prevented sinking of oxygenated surface water into the deep basins. Both freshening and increasing sea surface temperature (SST) of surface water are candidates to lower the density of surface waters. Whereas the close link between climate and sapropel formation is uncontested, the climatic trigger for hydrographic changes and sapropel formation is a matter of debate. The original hypothesis [*Olausson*, 1961] was that meltwater from the northern catchment triggered deep water stagnation in the late Quaternary, but has been challenged recently due to differences in timing of Black Sea flushing [*Lane-Serff et al.*, 1997; *Ryan et al.*, 1997]. This hypothesis also fails to explain the very regular temporal pattern of sapropels during the Pliocene and in the absence of ice on the Northern Hemisphere [*Hilgen*, 1991; *Lourens et al.*, 1996; *Rossignol-Strick*, 1983]. Alternatively, the northern catchment of the eastern Mediterranean Sea may have received increased precipitation during maximum insolation, leading to decreased salinity in the deep water formation areas [*Rohling and Gieskes*, 1989]. Recently, *Béthoux and Pierre* [1999] proposed that synchronous sapropel formation in the eastern and western Mediterranean Sea may be a consequence of decreased salinity of inflowing Atlantic surface water, reduced density of Mediterranean intermediate water forming in the eastern Mediterranean Sea, and reduced density difference of intermediate water masses at the Gibraltar Sill. Since approximately 600 kyr, sapropels were recorded under fully interglacial, fully glacial, and intermediate climate conditions (Figure 1), and correlation of sapropels with oxygen isotope curves shows that some sapropels (sapropels S6, S8 and some older ones) formed during glacials or cold stadials. In these ''glacial'' sapropels, microfossil and pollen assemblages indicate cold and arid conditions in the eastern Mediterranean area and global sea level was low [*Cita et al.*, 1977; *Rossignol-Strick*, 1983, 1985; *Rossignol-Strick et al.*, 1998; *Vergnaud-Grazzini et al.*, 1977]. Unfavorable for runoff from the northern catchment and for stratification, such conditions should also have increased the density contrast between Mediterranean and Atlantic water masses, and thus worked against deep water stagnation.

[5] Sapropel formation under glacial conditions is a strong argument for a source of freshwater in the monsoon system of Africa. It has been proposed that the salinity decrease may be due to greatly increased precipitation in the low-latitude southern catchment of the Nile River [*Rossignol-Strick*, 1983, 1985; *Rossignol-Strick et al.*, 1982]. In this hypothesis, sapropel formation would be closely linked to the strength of the African Monsoon and thus be connected to tropical and even southern hemisphere climate: the glacial sapropels S6 and S8 are seen to have formed in spite of unfavorable conditions in the Mediterranean [*Castradori*, 1993]. If true, this would make the Mediterranean Sea a unique recorder of tropical climate processes and their modulation by high-latitude influences. But the extent of freshwater discharge by the Nile river during some sapropel events is rather well constrained, suggesting that it was too small, or the effect too local, to alone explain the long-lasting enhanced stratification or the extent of isotope anomalies [*Béthoux*, 1993; *Foucault and Stanley*, 1989; *Jenkins and Williams*, 1983; *Krom et al.*, 1999; *Rohling and Bigg*, 1998; *Rohling and de Rijk*, 1999].

[6] A key issue in the discussion on the causes of stratification is to estimate the changes in SST and the changes of $\delta^{18}O_{seawater}$, frequently used to infer salinity decrease, as well as their timing in relation to sapropel formation. Early workers in the field recognized that sapropels coincide with significant isotopic depletion of ^{18}O in epiplanktonic foraminiferal calcite ($\delta^{18}O_{fc}$), a feature that indicates decreased $\delta^{18}O_{seawater}$ and decreased surface water salinity [*Fontugne and Calvert*, 1992; *Thunell and Williams*, 1989; *Vergnaud-Grazzini et al.*, 1977]. The large range of variations in $\delta^{18}O_{fc}$ (up to 5.5‰) in the late Quaternary eastern Mediterranean Sea [*Fontugne and Calvert*, 1992; *Thunell and Williams*, 1989; *Vergnaud-Grazzini et al.*, 1977] contrasts with open oceans records with only half that change. In the ocean, the variation is caused in part by the extraction and release of ^{18}O-depleted water by ice sheets (ice effect) [*Mix and Ruddiman*, 1984] and in part by sea surface temperature changes [*Epstein et al.*, 1953]. The larger than global range of $\delta^{18}O_{fc}$ in the eastern Mediterranean Sea is seen since the earliest Pliocene. It increased in the early Pleistocene with the onset of Northern Hemisphere glaciation and in particular since 600 kyr [*Kroon et al.*, 1998]. The large range reflects swings between a concentration basin (the modern Mediterranean) and either dilution by enhanced inflow of fresh water, or by inflow of isotopically depleted water prior to and during sapropel events [*Rohling*, 1999]. Change in SST also contributes in two ways: as an influence on the isotopic fractionation, and as a factor determining the density of seawater.

[7] We wished to explore the magnitude of change in $\delta^{18}O_{seawater}$, the possible influence of SST change on stratification, and the geographical patterns of these changes. For this, we analyzed the $\delta^{18}O_{fc}$ of the shallow-dwelling planktonic foraminifer *Globigerinoides ruber* (white) and SST on the same samples and in high temporal resolution over sapropels intervals in different basins of the eastern Mediterranean Sea. We compare the eastern Mediterranean

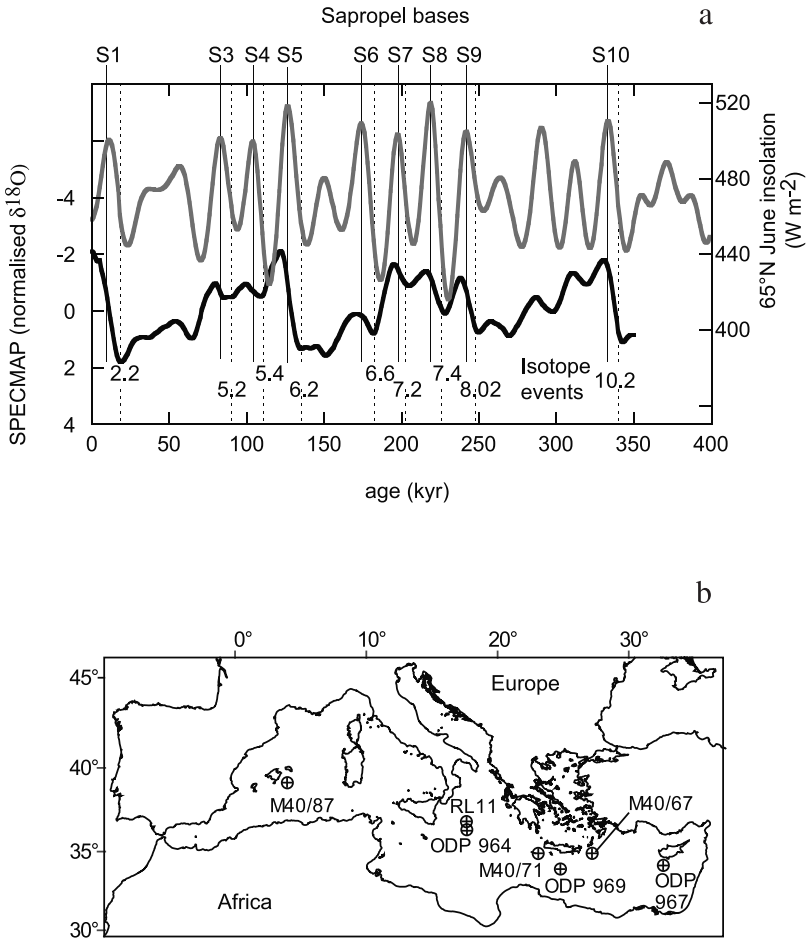

Figure 1. (a) Sapropel occurrence in relation to timing of the SPECMAP normalized $\delta^{18}O$ record showing glacial/interglacial cycles [*Imbrie et al.*, 1984] and summer insolation at 65°N [*Laskar et al.*, 1993]. (b) Map of sampling locations.

excursions in SST and $\delta^{18}O_{fc}$ to those found in a core from the Balearic Rise of the western Mediterranean Sea, which has no sapropel layers. Differing from previous studies [*Kallel et al.*, 2000, 1997; *Paterne et al.*, 1999], our paleo sea surface temperature estimates are based on the unsaturation ratio of long-chain ketones in lipid extracts ($U^{k'}_{37}$) that are used to correct $\delta^{18}O_{fc}$ for temperature effects. The unsaturation ratio of long-chain ketones $U^{k'}_{37}$ [*Brassell et al.*, 1986] in sedimentary lipids describes the relative abundance of diunsaturate and trunsaturated C_{37} alkenones that are produced by haptophyte algae, among them coccolithophores and their most prominent species *Emiliania huxleyi*. A recent inter-comparison experiment [*Rosell-Melé et al.*, 1998] and extensive field studies [*Müller et al.*, 1998] suggest that the method permits robust estimates of present and past SST over a wide range of environments and temperatures. With some caveats explained below, it is also applicable in the Mediterranean Sea [*Cacho et al.*, 1999a, 1999b; *Emeis et al.*, 2000b; *Ternois et al.*, 1997, 1996].

2. Materials and Methods

[8] Intervals comprising the sapropels S1 and S3 through S10 were sampled at 1 to 2 cm resolution from cores recovered by Ocean Drilling Program Leg 160 at Sites 969, and 967 (Figure 1; Table 1). In the Ionian Sea core at Site 964, only S1 and S8 were analyzed. Sample size restrictions and low concentrations of alkenones in non-sapropel samples precluded establishment of complete SST time series at the ODP sites, but most data sets include organic-poor muds below and above the individual sapropel layers. At the same resolution, tests of *Globigerinoides ruber* (white) were picked from the coarse fractions >63 μm and analyzed for $\delta^{18}O$ of calcite. Usually, 20 specimens were analyzed, but in some cases the number of specimens per sample decreased to <5 and yielded no reliable data. The isotope ratios are given relative to the PDB standard. Preparative and analytical methods for alkenone and isotope analyses are detailed in other papers [*Emeis et al.*, 1998, 2000b].

[9] All depths have been converted to revised meters composite depth (rmcd) [*Sakamoto et al.*, 1998] for the ODP sites, and only this depth is reported in tables and is used in the age assignments. To obtain continuous SST and $\delta^{18}O_{fc}$ estimates, we also analyzed gravity cores Meteor 40/4-71SL (western Mediterranean Ridge), -67SL (eastern Mediterranean Ridge) and -87SL (Balearic Rise in the western Mediterranean Sea), and trigger core Meteor 25-1/

Table 1. Sample Intervals Studied Here and Depths of Sapropel Intervals in Meters Below Seafloor[a]

					Sapropel Depth Interval		Interval Analyzed	
Sapropel	Location	Latitude	Longitude	Water Depth, m	Bottom, m	Top, m	Bottom, m	Top, m
No sapropels	M40/87	38°59.28′N	04°01.38′E	1913			5.51	0.01
S1	RL11	36°44.75′N	17°43.05′E	3376	0.43	0.31	0.57	0.29
	969	33°50.46′N	24°52.98′E	2201	0.33	0.27	0.35	0.16
	M40/71	34°48.67′N	23°11.63′E	2788	0.22	0.17	6.20	0.01
	M40/67	34°48.91′N	27°17.77′E	2158	0.21	0.12	5.48	0.01
	967	34°04.27′N	32°43.53′E	2550	1.30	1.18	1.71	0.94
S3	969				2.42	2.37	2.46	2.30
	M40/71				1.82	1.79		
	M40/67				2.52	2.39		
	967				4.32	4.24	4.45	4.16
S4	969				2.89	2.86	2.90	2.82
	M40/71				2.31	2.27		
	M40/67				3.20	3.15		
	967				5.63	5.38	5.68	5.24
S5	969				3.46	3.21	3.50	3.14
	M40/71				2.79	2.63		
	M40/67				4.61	3.65		
	967				7.69	7.43	7.77	7.36
S6	969				5.13	4.73	5.14	4.89
	M40/71				4.17	3.87		
	967				9.85	9.41	9.90	9.30
S7	969				5.62	5.47	5.63	5.53
	M40/71				4.66	4.55		
	967				10.92	10.71	11.19	10.69
S8	964	36°15.63′N	17°45.01′E	3660 m	12.90	12.70	13.00	12.56
	969				6.26	6.06	6.61	6.04
	M40/71				5.22	5.04		
	967				11.77	11.59	11.82	11.50
S9	969				no sapropel		6.61	6.04
	M40/71				5.63	5.57		
	967				12.23	12.17	12.29	12.09
S10	967				15.09	15.04	14.96	15.14

[a]Depths given for ODP Sites 964, 967, 969 are composite depths as given by *Sakamoto et al.* [1998].

RL11 taken in the Ionian Sea at the location of ODP Site 964 (see Table 1 and Figure 1). All cores were correlated by comparison of color (Minolta spectrophotometer) and physical properties measurements (GEOTECH MSCL) done at 2 cm intervals, and by comparison of SST and $\delta^{18}O$ curves. Isotope records of *G. ruber* are available for Sites 967 [*Kroon et al.*, 1998], 964, and 969 (Sakamoto, unpublished data).

[10] The calculation of SST from $U^{k'}_{37}$ relies on a linear relationship between unsaturation ratio and growth temperature of the haptophytes [*Prahl and Wakeham*, 1987]. Two linear relationships between sea surface temperatures and alkenone unsaturation ratios have been published for the Mediterranean Sea. The first is based on $Uk'37$ indices in 28 surface sediment samples and comparison to climatological SST [*Emeis et al.*, 2000b] and corresponds to the global relationship found by [*Müller et al.*, 1998]:

$$SST^{\circ}C = \left(U^{k'}_{37} - 0.044\right)/0.033,$$

which is virtually identical to the original equation [*Prahl and Wakeham*, 1987] based on cultures of *Emiliania huxleyi*. Another relationship

$$SST^{\circ}C = \left(U^{k'}_{37} + 0.21\right)/0.041$$

was found for suspended matter in the Northwestern Mediterranean Sea [*Ternois et al.*, 1997]. It yields higher temperatures and a lower range of SST. The different calibrations require reconciliation by additional work, but for reasons given elsewhere [*Emeis et al.*, 2000b] we use the global calibration to calculate SST in this paper. Below, the potential error resulting from an erroneous SST estimate will be briefly discussed. All analytical data will be deposited in the PANGEA data bank, or will be sent electronically upon request to the senior author.

[11] The stratigraphic position of upper Quaternary sapropels in the eastern Mediterranean Sea sequence has been established by radiocarbon dating of the youngest S1 [*Fontugne et al.*, 1994; *Troelstra et al.*, 1991], by comparison of stable isotope curves with those of oceanic environments [*Howell et al.*, 1998; *Kroon et al.*, 1998; *Rossignol-Strick*, 1983; *Vergnaud-Grazzini et al.*, 1977], by astronomical tuning of sapropel ages to insolation maxima [*Hilgen*, 1991; *Lourens et al.*, 1996; *Rossignol-Strick*, 1983] and by dating of tephra layers [*Kraml*, 1997; *Paterne et al.*, 1986].

[12] Using the sapropel mid points as age markers which have a constant lag of 3 kyr after the June insolation maximum at 65°N [*Hilgen*, 1991; *Lourens et al.*, 1996] is a simple and effective method, but may be too coarse when trying to unravel the exact timing of sapropels. Problems may originate from the only independent estimate of that lag, the age of the Holocene sapropel S1, and from post-depositional burn-down of the upper layers of sapropels, which would shift the physical midpoints to older ages [*Rossignol-Strick and Paterne*, 1999].

Table 2. Age Versus Depth of Stratigraphic Fix Points

Event	Age, kyr	Depth 967, rmcd	Depth 969, rmcd	Depth 964, rmcd	Depth M40-71, m	Depth M40-67, m	Depth M40-87, m[a]
Top	0	0.00	0.00		−0.14	−0.10	0.00
Base S1	9.5	1.30	0.37	0.43 (RL11)	0.22	0.21	0.23
2.2	18	1.72	0.56			0.47	0.65
4.22	64	3.37	1.87		1.43	1.95	2.58
Base S3	83	4.32	2.42		1.82	2.52	3.09
5.2	91	4.69	2.62		1.93	2.60	3.16
Base S4	105	5.63	2.89		2.31	3.20	3.49
5.4	111	5.96	3.02		2.35	3.25	3.54
Base S5	127	7.69	3.46		2.79	4.61	3.75
6.2	135	8.07	3.74		3.06	4.91	3.98
Top S6	170	9.41	4.73		3.89		4.41
Base S6	176	9.85	5.13		4.17		4.62
6.6	183	10.22	5.28		4.26		4.70
Base S7	197	10.92	5.62		4.70		5.00
7.2	201	11.24	5.71				5.07
Base S8	220	11.77	6.26	12.90	5.22		5.29
7.4	225	11.95					
Base S9	242	12.23	6.57		5.63		
8.02	248	12.48	6.94				
Base S10	334	15.09	7.76				
10.2	340	15.43	8.07				

[a]Sapropel equivalent depths based on comparison of isotope and temperature records.

[13] We aligned the bases of sapropels and plot our data in relation to that reference level. The reason is that the thickness and depths below seafloor of sapropel layers vary widely at the three coring locations. We then adjust the bases of each sapropel to the ages given in Table 2, which coincide with the maxima of the monsoon index and with maxima in Northern Hemisphere summer insolation in all cases but S4 [*Rossignol-Strick and Paterne*, 1999]. We reason that the initiation of sapropel deposition is the significant hydrographic event that must be compared with the peak of insolation to arrive at an age estimate that is independent of post-depositional effects. This fixing of the sapropel bases to maxima in insolation implies that the bases are isochronous, a view not shared by all workers [*Ströhle and Krom*, 1997]. The second implication is that the response of the eastern Mediterranean Sea to enhanced precipitation in the catchment is close to immediate. A lag of approximately 1 kyr between insolation maximum at low latitudes and the base of the sapropels is more likely [*Rossignol-Strick and Paterne*, 1999], but we chose to ignore this lag, which is difficult to quantify. We further use depths and ages of isotope events below sapropels [*Martinson et al.*, 1987] as additional fixed points in the age assignments (Table 2). For the time series, we then calculated ages for each sample by linear interpolation between the stratigraphic fix points. A problem in the age assignment for sapropel S6 is that the top of the sapropel yields ages that are too young to be reconciled with the age of ash layer V-0 above the organic-rich interval in cores from the Mediterranean Ridge and the Ionian Sea [*Keller et al.*, 1978]. The ash suggests that S6 is isochronous in the eastern Mediterranean [*Vergnaud-Grazzini et al.*, 1977]; it has recently been dated as 170 kyr ± 25 kyr [*Kraml*, 1997], with later measurements significantly reducing the age error (M. Kraml, personal communication, 1999). We thus added a stratigraphic fix point that sets the top of S6 to 170 kyr. This increases the sedimentation rate of S6 dramatically over that of surrounding muds, but because S6 is frequently laminated and is one of the few sapropels containing diatoms, we believe that the sedimentation rate increase in S6 may be real.

3. Results

[14] Figures 2a and 2b show the sediment lightness L*, isotope and SST curves versus age for all cores where continuous data sets are available. Crosses in the panels for ODP sites 969 and 967 indicate detailed measurements of $\delta^{18}O$ across sapropel intervals. At Site 964/RL11, only sapropels S1 and S8 are considered; whereas the S1 interval has been dated [*Emeis et al.*, 2000b], the S8 interval floats, because it is not covered by an existing continuous isotope curve at that site. However, S8 is well constrained in an isotope curve of *G. ruber* from nearby core KC01B [*Rossignol-Strick and Paterne*, 1999] showing that the amplitude of $\delta^{18}O_{fc}$ in the Ionian Sea is comparable to that of other basins. The range of $\delta^{18}O_{fc}$ is largest at Site 969 (−2.5‰ to 3.4‰) in the eastern basin; the western record has a range from −1.7‰ to 2.8‰. SST also vary strongly and range from 9C° to 21°C in the western and from 10°C to 25°C in the eastern records. The general features in the isotope records correspond to the standard isotope sequence in Figure 1a, although they are much spikier. An additional feature is the pronounced depletion within marine isotope stage 6 (around 150 kyr, between sapropels S6 and S5) that is not seen in the SPECMAP stack, and is only weak in the record from the western Mediterranean Sea (Figure 2a). The temperature records show that SST remained cold during that time (Figure 2b).

[15] Detailed profiles of SST and $\delta^{18}O_{fc}$ across the sapropel intervals (samples within sapropels are marked with filled symbols) are shown in Figure 3 on the depth scales adjusted to the bases of the sapropels. Deposition of sapropel S1 began during the early Holocene at approximately 9.5 kyr [*Emeis et al.*, 2000b; *Fontugne et al.*, 1994; *Troelstra et al.*, 1991] (Figure 3a) and followed a rapid

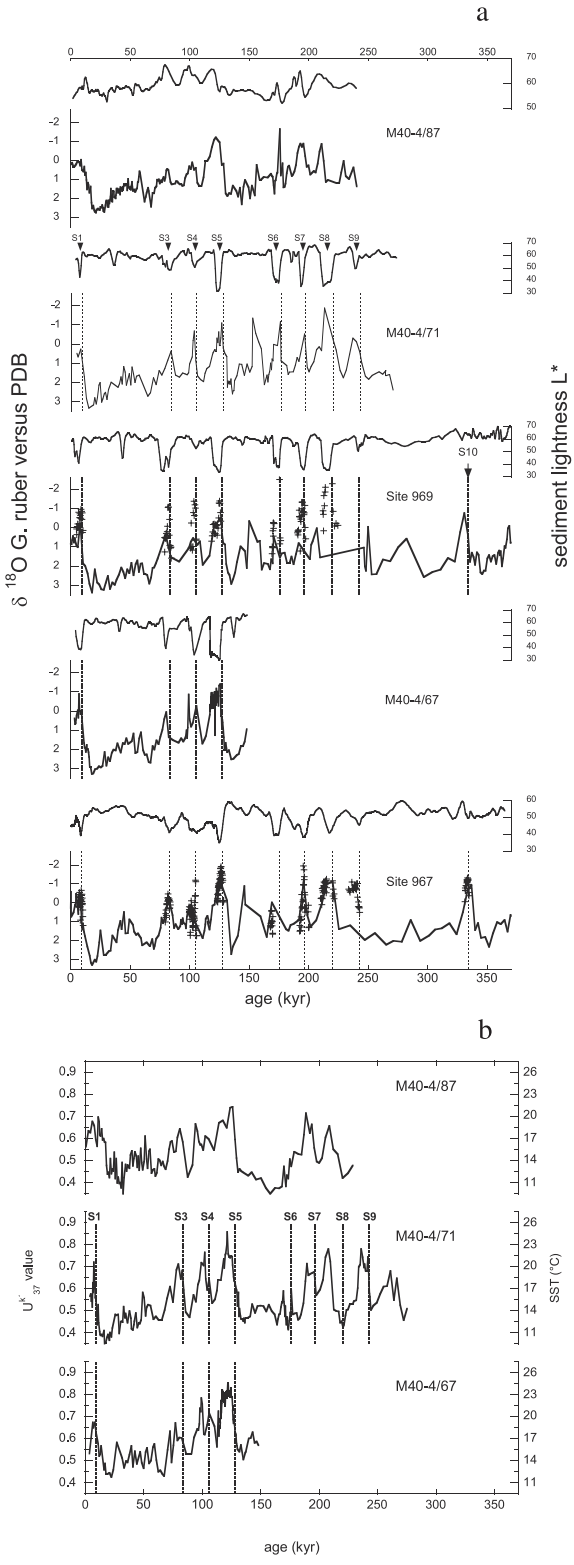

Figure 2. (a) The sediment lightness (L*) and isotope records of versus time. The sapropel intervals are marked S1 through S10. Crosses in the records from Sites 969 and 967 mark high-resolution analyses. (b) the temperature curves of the cores from the western Mediterranean Sea (M40-4/87) and the Mediterranean Ridge (M40-4/71 and M40-4/67).

warming phase at all locations. The average change in SST medians from isotope stage 2.2 below to within S1 is 2.5°C, the average decrease in $\delta^{18}O$ medians is 1.7‰ in the eastern Mediterranean records. The largest decrease in $\delta^{18}O_{fc}$ (−4.3‰ at ΔSST = 6.6°C) is seen on the western Mediterranean Ridge (ODP 969 and 71SL) and is 1.7‰ lighter and 2.1°C warmer than in the record from the western Mediterranean Sea.

[16] Sapropel S3 was deposited during isotopic substage 5a and its base is matched to the insolation maximum at 83 kyr. The median SST change is 1.7°C and $\delta^{18}O$ is depleted by 1.2‰; the maximum depletion (2.7‰ at ΔSST = 0.7°C) is again at Site 969 and is approximately 1.8‰ lighter than in the western Mediterranean where the SST change is considerably larger. The second of the sapropels in isotope stage 5 is S4, which has been set to begin at 105 kyr. In isotope records, it is correlated with the beginning of isotope substage 5c. The alignment of sapropel bases between the Levantine and Mediterranean Ridge records is tentative, because a sapropel doublet was found at Site 967, as is typical for cores from the Levantine Basin [*McCoy*, 1974]. The largest change is again recorded on the Mediterranean Ridge with a maximum decrease of 3.3‰ in $\delta^{18}O$ accompanied by a rise in SST of 2.9°C. The Balearic Rise has a decrease of 1.3‰ and a warming of 2°C.

[17] Sapropel S5 is correlated with isotope substage 5e and with the beginning of the Eemian. SST rise from below 15°C in isotope stage 6 to more than 20°C at the top of the organic rich layer. In all records we note a decrease in $\delta^{18}O$ some centimeters below the base of the sapropel (Figure 3d). The median SST increase is 8.7°C and accompanies a decrease by 2.7‰ in $\delta^{18}O$. This moderate average isotopic depletion reflects the lack of data for the full glacial isotope stage 6 in the Levantine Basin Site 967. Nonetheless, this site still has the maximum depletion in our data (4.6‰) at a rise of 6.7°C in SST. Maximum depletion in the western Mediterranean is 3.5‰ at ΔSST = 8.9°C.

[18] The SST records of sapropel S6 are unique, because the sea surface cooled during the sapropel interval (Figure 3e). Only four samples within the basal S6 contained specimens of *G. ruber* for measurement of $\delta^{18}O$, the centers of the S6 intervals were barren. At Site 969, one measurement at 1 cm above the base was 0.8‰, one at 2 cm above the base was −2.5‰. The moderate isotope depletion of 1.4‰ suggested by the medians (based mainly on the data points from the top of S6) is certainly too low, and that between minimum and maximum at Site 969 (4.3‰ associated with a temperature decrease of 2.1°C) is more likely to reflect the magnitude of isotopic depletion of the surface layer. *G. bulloides* records from the Ionian Sea [*Schmiedl et al.*, 1998] and the Mediterranean Ridge [*Thunell et al.*, 1983] have depletions of 3‰ and 2.6‰, respectively. The record from the western basin has a depletion of 3.1‰ of *G. ruber* calcite at SST that cooled by 1.6°C.

[19] Sapropel S7 (Figure 3f) was deposited at the end of interglacial stage 7 (substage 7a) and its base is matched to the insolation maximum at 197 kyr. The median $\delta^{18}O$ ratios decreased by 1.1‰ from below to the center of the sapropel at invariant temperatures, but minima and maxima in $\delta^{18}O$ differ by 3‰ and by 3.5°C in SST at Site 969. The coeval

change in the western basin was −1.5‰ in $\delta^{18}O$ and a warming of 2.1°C. Orbital tuning aligns the base of S8 with insolation cycle 20 at 220 kyr. It began to form during the brief and intensely cold isotope stage 7d with basal temperatures that are as low as 13°C. SST warmed rapidly during the sapropel period and reached between 18 and 20°C toward the top (Figure 3g). As was the case with S6, the planktonic foraminifer *G. ruber* is absent in most samples from the bases of S8. At Site 969, *G. ruber* shows a decline in $\delta^{18}O$ from −0.1‰ to −2.3‰. After the barren interval, $\delta^{18}O$ begins at −2‰. We also measured the $\delta^{18}O$ of *G. bulloides*, which yielded specimens in all S8 samples at Sites 964 and 967 (Figure 3g). Both records show very high variability within S8, but most heavy values below the base are 1.5‰ and decrease to −0.5‰ within the sapropel. At the location in the Levantine Basin, $\delta^{18}O$ decrease over almost 1.5‰ from 1 cm below to within the sapropel, whereas the change in the Ionian Sea record is more gradual. The median decrease in $\delta^{18}O$ is 1‰ in *G. ruber*, accompanied by 2° warming. Maximum decrease in $\delta^{18}O$ is 2.2‰ at Site 969 at ΔSST = 1.7°C. We aligned the SST record of SL87 with those of the eastern Mediterranean Sea for correlation (Figures 2a and 3g) and find that the SST and isotope records are offset by several cm. Barring a misalignment, the $\delta^{18}O$ change in the western basin associated with S8 deposition was −1.5‰ and SST warmed by 0.8°C. Two sapropels (S9 and S10) were only analyzed at Site 967 and in core M40/71. The maximum decrease in $\delta^{18}O$ is 1.9 and 1‰, respectively, accompanied by SST increases of 4° and 2°C (Table 3).

[20] In summary, the development of conditions in the sea surface before and during individual sapropel periods was very similar at all locations in the eastern Mediterranean Sea. The $\delta^{18}O_{fc}$ decreased in all cases some centimeters below or at the sapropel base. Most sapropels show a warming coincident with or slightly lagging the lowered $\delta^{18}O_{fc}$ values. An exception to this pattern is sapropel S6, which exhibits cooling within the organic-rich layer. In all cases, the isotopic depletion of records in the eastern basins significantly exceeded that of the western basin. We also note that most significant depletions in $\delta^{18}O$ apparently occurred in the vicinity of the Mediterranean Ridge, except in the cases of S5 and S7, which are most depleted in the Levantine Basin.

4. Discussion

[21] After discussing possible errors, we use our data to estimate the change $\delta^{18}O_{seawater}$ associated with each sapropel event in the eastern Mediterranean Sea and to search for spatial gradients. By comparing the estimates of SST and $\delta^{18}O_{seawater}$ with the record from the western Mediterranean Sea, with climatic indicators of monsoon strength, ice volume, and insolation, we hope to identify the footprints of possible influences on hydrography in the eastern Mediterranean Sea. Finally, we use the combined isotopic and SST records to shed light on the possible causes for "glacial" sapropels S6 and S8.

4.1. Error Estimates

[22] Two regressions between SST and $U^{k'}_{37}$ exist for the Mediterranean Sea [*Emeis et al.*, 2000b; *Ternois et al.*, 1997] that differ in slope. Notably, the regression of Ternois and coworkers causes increasingly higher temperature estimates in the low $U^{k'}_{37}$ range. The maximum error, which we risk by using the global calibration [*Müller et al.*, 1998] to calculate the temperature difference between the warmest sample ($U^{k'}_{37}$ = 0.85) and the coldest sample in stage 6 of core M40-4/67 ($U^{k'}_{37}$ = 0.43), is 2.3°C. For the intervals preceding and in sapropels, the maximum discrepancy is 1.1°C for S1 and S5. For the other intervals, it is below the analytical error estimated at 0.5°C. Our range of temperatures agree well with the range of SST reconstructed from foraminifer assemblages [*Emeis et al.*, 2000b; *Ternois et al.*, 1997], but the detailed patterns differ significantly from their less resolved reconstructions. A further error in our SST estimates may arise from a variable overprint of the alkenone unsaturation patterns by diagenesis under oxic and anoxic conditions [*Gong and Hollander*, 1999; *Hoefs et al.*, 1998; *Prahl et al.*, 1989]. *Gong and Hollander* [1999] found a systematic offset between SST estimates from coeval laminated and neighboring nonlaminated sediments. The SST estimates of anoxic sediments were found to be colder by 2.5°C, attributed to bioturbation and a possible preferential degradation of the triunsaturated relative to the diunsaturated C_{37} methyl ketones under oxic conditions. Their interpretations are in line with arguments presented by *Hoefs et al.* [1998], but contradict earlier studies [*Prahl et al.*, 1989] that found no evidence for preferential degradation. Our detailed data across oxic/anoxic transitions at the bases of the sapropels show a temperature decrease (expected from diagenetic bias) only in the case of S6 (Figure 3e). All other transitions are marked by a temperature change in the opposite sense of that expected from diagenesis, and no transition (except S6 which is discussed below) shows abrupt offsets in the SST estimates. A second reason for our opinion that diagenesis has not affected the alkenone unsaturation ratios is the case of S9, which is an anoxic sapropel at Site 967, but is not present at Site 969 due to post-depositional oxidation. The temperature curves for both sequences are identical (Figure 3h). However, the evidence remains circumstantial for the resilience of the $U^{k'}_{37}$ against diagenesis. Should a systematic diagenetic change have caused raised $U^{k'}_{37}$ (and higher calculated SST) of oxic sediments, then the estimates of temperature differences between underlying oxic muds and sapropels become greater. The effect on $\delta^{18}O_{fc}$ and on the reconstructed $\delta^{18}O_{seawater}$ of a 2°C underestimation of the SST difference between samples below and within sapropels would be −0.4‰.

[23] Potentially more serious is a systematic error that we introduce into our calculations by using only one species of planktonic foraminifers [*Tang and Stott*, 1993], and one that has a different growth season than the haptophytes which produce the temperature signal. The SST estimate from alkenones is biased toward SST during the bloom period of coccolithophores, which in the eastern Mediterranean Sea is during late winter/early spring [*Ziveri et al.*, 2000]. *G. ruber* appears to be most abundant under summer/fall stratified conditions [*Pujol and Vergnaud-Grazzini*, 1995]. We thus probably underestimate the growth temperature effects on $\delta^{18}O_{calcite}$ of *G. ruber*. However, we feel that this is a systematic error that applies to both the western and the

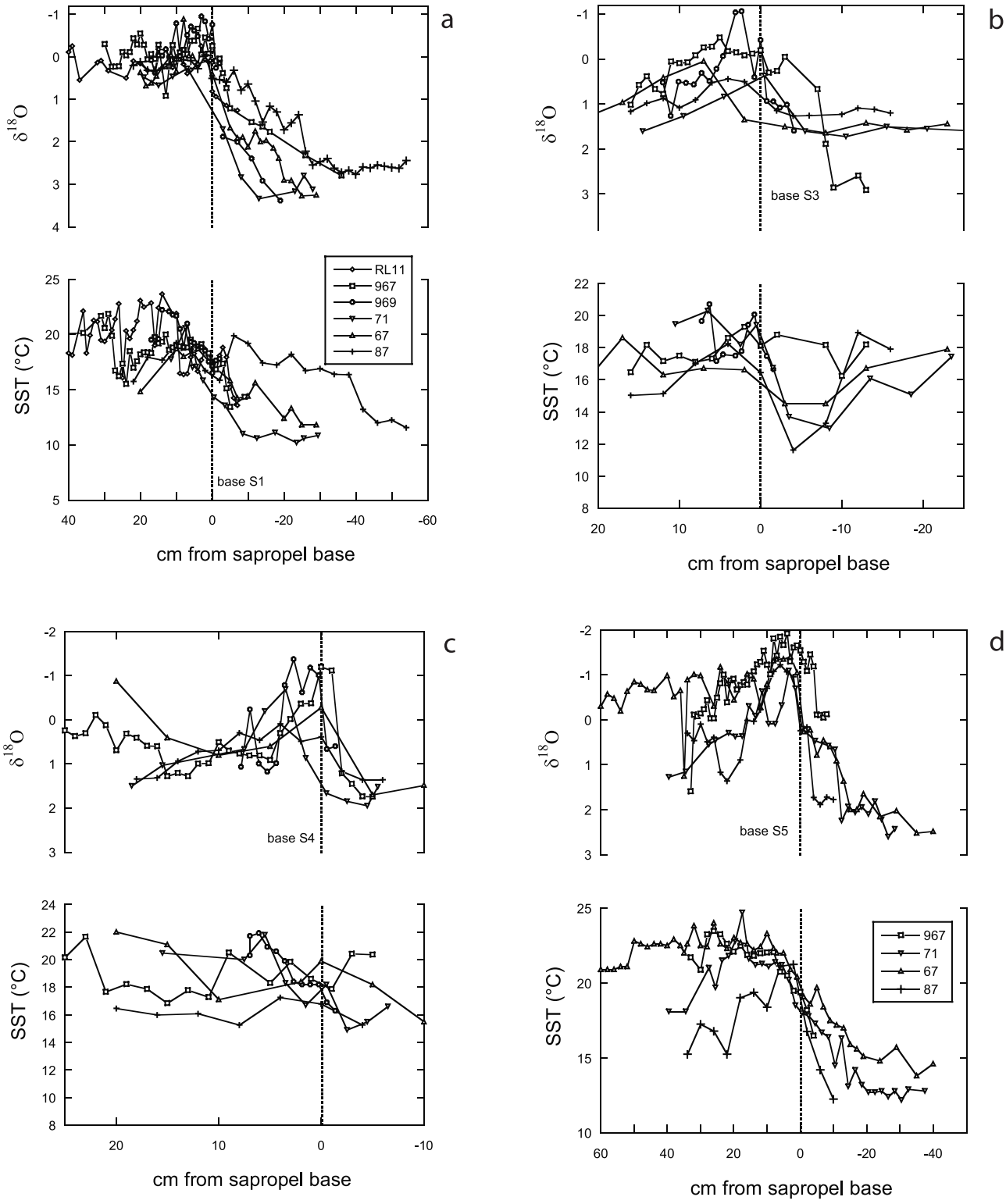

Figure 3. Detailed records of $\delta^{18}O$ *G. ruber* (white) and SST for sapropels S1 (a), S3 (b), S4 (c) S5 (d), S6 (e), S7 (f), S8 (g), S9 (h) and S10 (i) versus depth relative to the sapropel bases. The panel for S8 (Figure 3g) also shows the more complete records of $\delta^{18}O$ for *G. bulloides.*

eastern Mediterranean Sea. Inspection of relationships between annual average SST at 5 m water depth (from the Mediterranean Oceanographic Database) [*Brasseur et al.*, 1996] versus average summer/fall and winter/spring SST show that the relationships are linear in both basins and are not biased by E-W differences. We have no basis for speculations that the linear relationships between SST in different seasons in the two basins did not hold for past conditions.

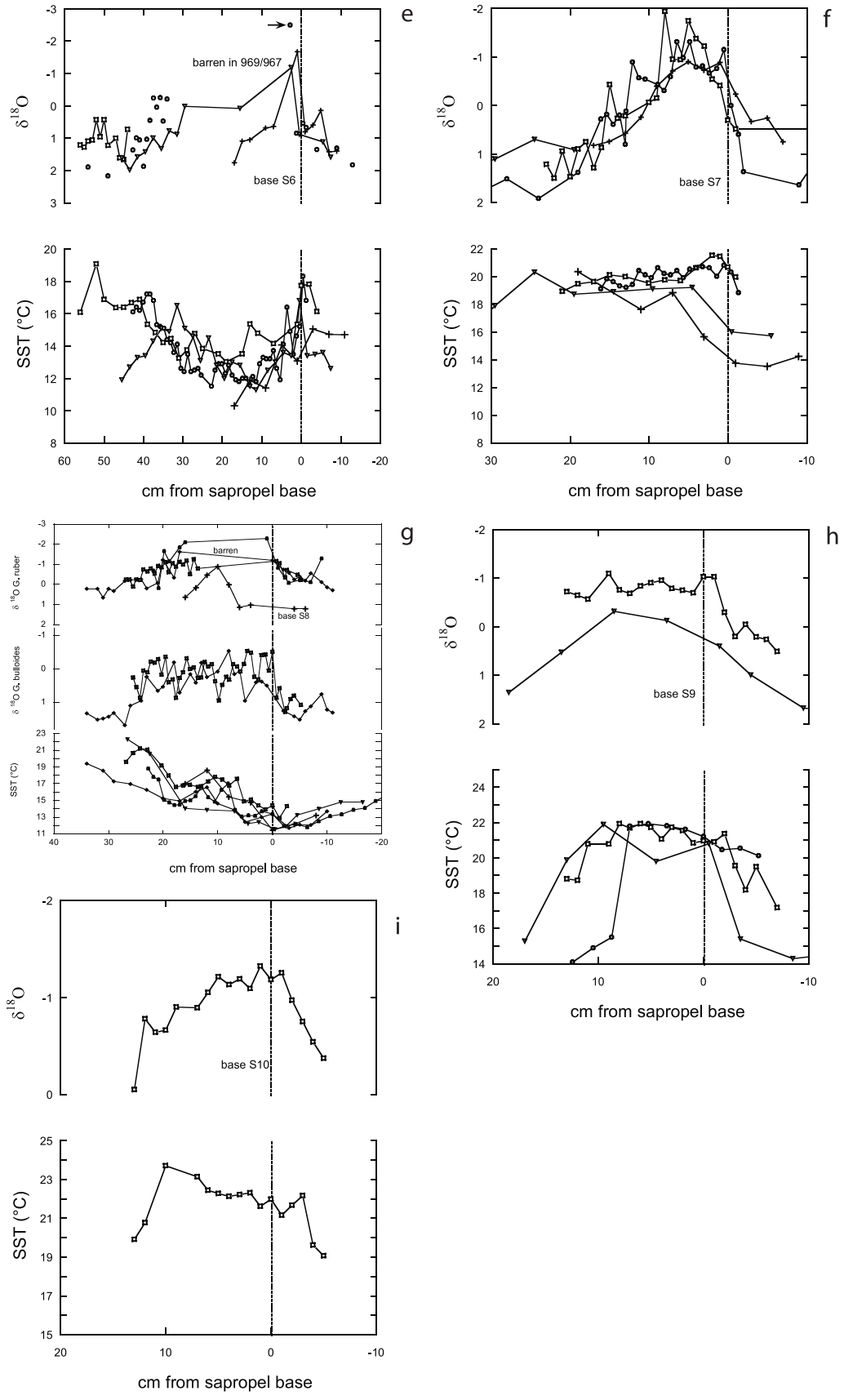

Figure 3. (continued)

Table 3. $\delta^{18}O$ and Uk′37 Determinations and Estimated SST From the Calibration of *Müller et al.* [1998] (SST M) and *Ternois et al.* [1997] (SST T) for Time Intervals Bracketing the Sapropel Events and From the Base of the Sapropels to the Preceding Glacial/Stadial Event[a]

Sapropel	Event	Core	Age,[b] kyr	$\delta^{18}O$	N	±1σ	Uk′37	N	±1σ	SST M^2	SST T^2	$\delta^{18}O$ Min/Max	SST Min/Max	Age Min/Max	Remarks
		M40/87	*7–9.5*	*0.19*	*4*	*0.24*	*0.63*	*2*	*0.04*	17.7	20.4	*0.0*	*16.7*	*8.9*	
S1		RL11		0.18	10	0.36	0.62	11	0.03	17.3	20.1	−0.3	17.7	8.5	
		M40/71+969		−0.61	11	0.29	0.67	11	0.05	18.9	21.4	−1.0[b]	18.4[b]	9.2[b]	
		M40/67		0.07	5	0.17	0.65	2	0.03	18.3	21.0	0.0	18.7	7.8	
		967		−0.11	23	0.32	0.66	22	0.02	18.8	21.3	−0.7	18.8	9.1	
Below S1	*2.2*	*M40/87*	*9.5–18*	*1.56*	*21*	*0.85*	*0.60*	*11*	*0.06*	16.9	19.8	*2.6*	*13.2*	*18.0*	
		RL11		1.20	2	0.08	0.59	6	0.07	16.6	19.5	1.3	13.6	10.6	LGM not reached
		M40/71+969		2.01	7	1.24	0.63	2	0.00	17.7	20.4	3.4[b]	11.8[b]	18.0[b]	SST from SL67
		M40/67		2.06	12	0.52	0.52	7	0.05	14.5	17.9	3.3	11.8	17.7	
		967		1.37	10	1.11	0.56	6	0.08	15.6	18.7	3.2	11.8	17.2	SST from SL67
Change in western Mediterranean				**−1.38**			***0.03***			***0.8***	***0.6***	***−2.6***	***3.5***		
Change in eastern Mediterranean				**−1.71**			**0.08**			**2.5**	**2.0**	**−4.3**	**6.6**		
		M40/87	80–83	*0.48*	*2*	*0.04*	*0.62*	*2*	***0.04***	*17.3*	*20.1*	*0.5*	*18.2*	*80.7*	
S3		M40-71		0.61	2	0.33	0.66	2	0.03	18.8	21.3	0.4	19.4	83.5	SST interpolated
		969		−0.24	6	0.63	0.63	7	0.04	17.8	20.5	−1.1[b]	17.4[b]	82.2[b]	
		M40/67		0.24	2	0.26	0.60	2	0.01	16.8	19.7	0.1	16.7	80.4	
		967		−0.08	17	0.42	0.62	9	0.03	17.5	20.3	−0.5	17.9	82.0	
Below S	5.2	*M40/87*	*83–91*	*1.26*	*3*	*0.07*	*0.43*	*1*		*11.6*	*15.5*	*1.3*	*11.6*	*87.6*	
		M40/71		1.67	2	0.08	0.50	3	0.07	13.7	17.2	1.7	13.0	90.0	
		969		1.02	5	0.28	0.61	2	0.02	17.0	19.9	1.6[b]	16.7[b]	84.6[b]	SST from SL71
		M40/67		1.51	3	0.15	0.53	3	0.04	14.8	18.1	1.6	14.5	90.6	
		967		0.48	8	0.57	0.62	2	0.06	17.5	20.3	1.4	14.5	90.4	SST from SL67
Change in western Mediterranean				***−0.78***			***0.19***			***5.7***	***4.6***	***−0.8***	***6.6***		
Change in eastern Mediterranean				**−1.19**			**0.06**			**1.7**	**1.4**	***−2.7***	***0.7***		
		M40/87	*100–105*	*0.39*	*4*	*0.18*	*0.58*	*2*	*0.05*	16.2	19.3	*0.1*	*17.2*	*102.6*	
S4		M40-71		0.24	4	0.73	0.68	4	0.07	19.2	21.6	−0.7	18.3	103.0	
		969		−0.42	10	1.04	0.72	10	0.05	20.6	22.8	−1.4[b]	18.4[b]	103.8[b]	
		M40/67		0.96	2	0.06	0.62	3	0.02	17.5	20.3	0.9	17.7	102.8	
		967		0.59	33	0.58	0.65	16	0.05	18.5	21.0	−1.2	18.6	105.0	
Below S4	5.4	*M40/87*	*105–111*	*1.17*	*3*	*0.51*	*0.57*	*2*	*0.04*	*16.0*	*19.1*	*1.4*	*15.2*	*109.8*	
		M40-71		1.85	3	0.14	0.55	3	0.06	15.5	18.6	2.0	15.5	110.7	
		969		0.72	5	0.56	0.60	2	0.15	16.9	19.8	1.9[b]	15.5[b]	111.0[b]	SST from SL71
		M40/67		0.65	2	0.57	0.69	2	0.04	19.5	21.9	1.1	18.2	110.6	
		967		1.46	5	1.20	0.72	3	0.05	20.4	22.6	1.8	20.4	105.9	
Change in western Mediterranean				***−0.78***			***0.01***			***0.2***	***0.2***	***−1.3***	***2.0***		
Change in eastern Mediterranean				**−0.67**			**0.02**			**0.6**	**0.5**	***−3.3***	***2.9***		
		M40/87	122–127	*−1.07*	*5*	*0.60*	*0.74*	*2*	*0.00*	21.2	23.2	*−1.2*	*21.1*	*123.8*	
S5		M40-71		−0.31	8	0.42	0.74	8	0.03	21.2	23.3	−1.1	20.2	125.9	
		969		no data											
		M40/67		−0.86	16	0.66	0.80	18	0.05	22.8	24.6	−1.4	20.9	125.6	
		967		−0.94	32	0.57	0.77	15	0.04	22.0	23.9	−1.9[b]	20.5[b]	126.5[b]	
Below S5	6.2	*M40/87*	*127–135*	*1.74*	*10*	*0.57*	*0.46*	*6*	*0.06*	*12.5*	*16.3*	*2.3*	*12.2*	*134.7*	
		M40-71		1.94	12	0.84	0.52	14	0.07	14.3	17.7	2.6	12.4	134.9	
		969		no data											
		M40/67		1.83	10	0.70	0.58	10	0.05	16.2	19.2	2.5	13.8	135.0	
		967		−0.60	10	1.26	0.65	5	0.04	18.2	20.9	2.7[b]	13.8[b]	135.0[b]	SST from SL67
Change in western Mediterranean				***−2.81***			***0.29***			***8.7***	***7.0***	***−3.5***	***8.9***		
Change in eastern Mediterranean				**−2.68**			**0.19**			**5.9**	**4.7**	***−4.6***	***6.7***		
		M40/87	*170–176*	*0.85*	*12*	*0.82*	*0.42*	*9*	*0.05*	*11.4*	*15.4*	*−1.7*	*13.1*	*176.0*	
S6		M40-71		0.08	3	1.04	0.47	15	0.05	13.0	16.7	−1.2	13.4	175.4	
		969		−0.82	2	2.36	0.48	21	0.05	13.1	16.8	−2.5[b]	14.9[b]	175.6[b]	

Table 3. (continued)

Sapropel	Event	Core	Age,[b] kyr	$\delta^{18}O$	N	±1σ	$Uk'37$	N	±1σ	SST M^2	SST T^2	$\delta^{18}O$ Min/Max	SST Min/Max	Age Min/Max	Remarks
		967		1.20	2	0.66	0.53	23	0.05	14.8	18.1	barren at base			
Below S6	6.6	*M40/87*	*176–183*	*0.70*	*4*	*0.53*	*0.54*	*2*	*0.01*	*14.9*	*18.2*	*1.4*	*14.7*	*182.1*	
		M40-71		1.46	3	0.24	0.49	5	0.01	13.4	17.0	1.6	12.6	181.8	
		969		1.33	6	0.50	0.64	2	0.04	17.9	20.6	1.8[b]	12.6[b]	181.8[b]	SST from SL71
		967		1.44	2	0.05	0.63	3	0.03	17.7	20.5	1.5	12.8	183.0	SST from SL71
Change in western Mediterranean				***0.15***			***−0.12***			***−3.5***	***−2.8***	***−3.1***	***−1.6***		
Change in eastern Mediterranean				**−1.36**			**−0.15**			**−4.6**	**−3.7**	***−4.3***	***−2.1***		
		M40/87	191–197	−0.72	*6*	*0.43*	*0.63*	*3*	*0.05*	17.6	20.4	*−0.7*	*15.6*	195.4	
S7		M40-71		−0.53	1		0.67	3	0.00	19.1	21.5	−0.5	19.2	195.6	
		969		−0.63	18	0.65	0.72	18	0.02	20.6	22.8	−1.3	20.5	194.9	
		967		0.08	22	1.06	0.70	13	0.04	19.7	22.1	−1.7[b]	20.2[b]	196.1[b]	
Below S7	7.2	*M40/87*	197–201	*0.30*	*4*	*0.40*	*0.49*	*2*	*0.01*	*13.6*	*17.2*	*0.8*	*13.5*	*199.9*	interpolated SST
		M40-71		1.33	2	0.16	0.58	2	0.02	16.4	19.4	1.4	16.8	199.2	
		969		0.99	4	0.75	0.70	2	0.04	20.0	22.3	1.6	16.7	201.0	SST from SL71
		967		0.66	3	0.40	0.70	1		19.9	22.2	1.3[b]	16.7[b]	201.0[b]	SST from SL71
Change in western Mediterranean				***−1.01***			***0.13***			***4.0***	***3.2***	***−1.5***	***2.1***		
change in eastern Mediterranean				**−1.52**			**−0.01**			**−0.2**	**−0.2**	***−3.0***	***3.5***		
		M40/87	213–220	*1.03*	*3*	*0.85*	*0.48*	*2*	*0.08*	*13.1*	*16.7*	*−0.4*	*12.9*	*217.9*	interpolated SST
S8		964		−1.20	4	0.54	0.53	9	0.05	14.6	18.0	−1.2	13.4	220.0	
		M40/71		−1.87	1		0.50	5	0.03	13.7	17.2	−1.9[b]	16.2[b]	213.4[b]	
		969		−1.40	8	0.83	0.54	20	0.05	15.0	18.2	−2.3	13.4	219.8	
		967		−1.00	11	0.23	0.61	17	0.05	17.1	20.0	−1.3	17.1	215.3	
Below S8	7.4	*M40/87*	220–225	*1.21*	*1*		*0.44*	*1*		*12.0*	*15.9*	*1.2*	*12.1*	*224.2*	
		964		−0.24	9	0.34	0.44	4	0.03	12.1	15.9	0.2	13.7	222.0	
		M40/71		1.37	1		0.46	4	0.04	12.6	16.3	1.4[b]	14.0[b]	225.0[b]	
		969		−0.16	4	0.36	0.45	4	0.02	12.3	16.1	−0.1	11.7	221.9	
		967		−0.60	6	0.38	0.57	4	0.08	15.9	19.0	−0.2	17.2	221.3	
Change in western Mediterranean				***−0.18***			***0.04***			***1.1***	***0.9***	***−1.6***	***0.8***		
Change in eastern Mediterranean				**−1.10**			**0.08**			**2.3**	**1.9**	***−3.2***	***2.2***		
S9		M40/71	239–242	−0.22	2	0.13	0.73	2	0.02	20.8	22.9	−0.1[b]	19.8[b]	239.0[b]	
		967		−0.76	10	0.43	0.74	10	0.04	21.0	23.1	−1.0	21.0	240.6	
	8.2	M40/71	242–248	1.63	5	0.59	0.55	4	0.03	15.3	18.5	1.8[b]	14.7[b]	248.0[b]	
Below S9		967		0.40	4	0.82	0.65	2	0.05	18.3	21.0	0.5	17.2	243.0	
Change in eastern Mediterranean				**−1.5**			**0.1**			**4.0**	**3.3**	**−1.9**	**5.1**		
S10		967	332–334	−0.99	14	0.34	0.78	12	0.03	22.2	24.1	−1.3	21.6	333.7	
Below S10	10.2	967	334–340	−0.65	6	0.96	0.74	5	0.04	21.2	23.2	−0.4	19.6	334.9	
Change in eastern Mediterranean				***−0.34***						***1.0***	***0.8***	***−1.0***	***2.0***		

[a]Given are values for each core, including standard deviations (± 1σ) and number of samples (N), and the median change of all cores considered (in boldface). $\delta^{18}O$ Min/Max are the maximum depletions seen from below to within the sapropels, SST Min/Max is the corresponding change in SST for the same samples (based on the *Müller et al.* [1998] calibration), and age Min/Max is the assigned age for these samples. Lines in italics denote the data for the western Mediterranean core M40/87.

[b]The core with the largest $\delta^{18}O$ depletion for each individual sapropel cycle.

[24] By using the $U^{k'}_{37}$ calibration based on annual average SST, we effectively halve the error caused possibly by different growth seasons. Based on regression equations between climatological summer/fall and winter/spring SST at 5 m water depth, respectively, with annual average SST and the range of SST found in our data set for past conditions at peak isotopic depletion (maximum of 20.5°C in the case of S5), we estimate the maximum error incurred by using annual average SST at 2.8°C, equivalent to 0.56‰ $\delta^{18}O$. Because we are interested in relative changes at glacial-interglacial transitions, this error is substantially reduced by subtracting the error at minimum SST (in the case of S5, this is equivalent to MIS6.2 with 13.8°C, potential SST error estimated at 2.2°C, which is equivalent to 0.44 ‰ $\delta^{18}O$) from that at maximum depletion at the sapropel bases and arrive at a maximum error derived from seasonal offsets of SST and $\delta^{18}O_{fc}$ signals at ±0.12‰ $\delta^{18}O$ for the transition from MIS6.2 to S5. This is well covered by our overall error

estimate of 0.5‰. Furthermore, this error will be systematic and affects all records in the same way.

[25] The error associated with the estimates of $\delta^{18}O_{seawater}$ change (disregarding the questionable diagenetic effect of $U^{k'}_{37}$) is a composite of measurement errors of $U^{k'}_{37}$ (0.5°C or 0.1‰ in $\delta^{18}O$), of SST calibration errors (1.5°C or 0.3‰ in $\delta^{18}O$) [*Müller et al.*, 1998], of errors in the determination of $\delta^{18}O$ (<0.1‰), and the average of $\delta^{18}O_{fc}$ errors for individual time slices. The average error estimate is ±0.5‰ for $\delta^{18}O_{seawater}$, in line with previous investigations [*Paterne et al.*, 1999].

4.2. Temperature and $\delta^{18}O$ Variations Associated With the Onset of Sapropel Conditions

[26] Based on the data displayed in Figure 3, we calculated median values of SST and $\delta^{18}O_{fc}$ during and before sapropel events for each location (Table 3). The curves in Figure 3 suggest, however, that the medians of values below and within sapropels do not capture the larger ranges of both properties. Table 3 thus also lists minima and maxima of $\delta^{18}O_{fc}$ for each sapropel interval, the alkenone temperature estimate corresponding to the same samples, and their ages. In most cases, the alkenone temperatures were determined on the same sample; in those samples with maximal $\delta^{18}O_{fc}$ that do not have a temperature estimate, we used the coeval temperature estimate from the nearest continuous record. Continuous records of temperature (Figure 2b) suggest that the glacial-interglacial temperature change in the eastern Mediterranean Sea was close to 10°C. This is large in comparison to open-ocean SST records of alkenone temperatures from the same latitudes [*Bard et al.*, 1997; *Doose et al.*, 1997; *Emeis et al.*, 1995; *Rostek et al.*, 1997; *Schneider et al.*, 1995; *Sonzogni et al.*, 1997; *Zhao et al.*, 1995], but agrees with estimates from the North Atlantic Ocean between 40° and 50° latitude [*Madureira et al.*, 1997; *Villanueva et al.*, 1998] and a recent estimate of SST change in the Alboran Sea [*Cacho et al.*, 1999b]. The original estimates of glacial/interglacial SST change based on isotopes [*Cita et al.*, 1977] were 5.5°C (stage 10/9), 3°C (stage 8/7), 8°C (stage 6/5) and 4°C (stage 2/1), and are well matched by our data, as is the upper range of temperature change (11°C) postulated by *Vergnaud-Grazzini* [1975]. In their reconstruction of salinity change associated with S1, *Thunell and Williams* [1989] estimated that the eastern Mediterranean basin was 4°C colder during the LGM as compared to modern. On land, temperature changes were considerably larger. Based on a lacustrine pollen record from southern Italy, *Allen et al.* [1999] estimated that the temperature of the coldest month fluctuated by as much as 20°C over the last glacial period with high temporal variability. Foraminifer assemblages [*Kallel et al.*, 1997] suggest a rapid increase in SST (10°C) at the end of the last glacial maximum, whereas numerical climate simulations [*Bigg*, 1995] produce temperatures that were lower by 5°C in the Mediterranean Sea in winter and by 1 to 6°C in summer during the last glacial maximum.

[27] The range of $\delta^{18}O_{fc}$ in our records also recapitulates previous estimates [*Fontugne and Calvert*, 1992; *Rossignol-Strick and Paterne*, 1999; *Schmiedl et al.*, 1998; *Vergnaud-Grazzini et al.*, 1977]. The isotope depletion at the stage 6/S5 transition and the stage2/S1 transition is 4.6‰ and 4.3‰, respectively, when using maxima and minima. A detailed survey of records bracketing LGM and S1 [*Rohling and de Rijk*, 1999] gave a depletion of 3.4‰ in the eastern basin except for the Levantine Basin where it is 4.2‰.

[28] Table 4 compiles the median and maximal values of ΔSST and $\Delta\delta^{18}O$ (difference from before to within the sapropels). We included the medians in this compilation, because they may be compared to results from previous and future low-resolution studies. Using a temperature factor [*Epstein et al.*, 1953] of 0.2‰ per 1°C to calculate the effect of temperature on the fractionation between $\delta^{18}O_{seawater}$ and $\delta^{18}O_{fc}$, we find that ΔSST contributes between +0.9‰ to −1.2‰ (medians) and +0.4‰ to −1.3‰ (maxima/minima) to $\Delta\delta^{18}O_{fc}$ and thus significantly influenced the $\delta^{18}O$ variations. In addition to regional SST change, the global ice effect has to be subtracted from the local record, for which we use the data set of *Vogelsang* [1990] (Table 4). The ice effect was highest prior to and during S5 (−1.24‰) and lowest during S7 (−0.1‰). This global effect further reduces the portion of $\Delta\delta^{18}O_{fc}$ attributed to $\delta^{18}O_{seawater}$ change, estimates for which are also listed in Table 3. Estimated changes in $\delta^{18}O_{seawater}$ associated with sapropels range from +0.4‰ (S10) to −3.2‰ (S6) in the median estimates. The changes based on maximal/minimal $\delta^{18}O_{fc}$ are between −0.6‰ (S10) and −3.0‰ (S6).

[29] The temperature and ice volume corrections significantly reduced the large $\Delta\delta^{18}O_{fc}$ associated with sapropels, and in most median estimates (except S6 and S7) to within the estimated error margin of 0.5‰. After corrections, all median $\Delta\delta^{18}O_{seawater}$ estimates (except those of S6 and S7; Table 4) also are in the same range as $\Delta\delta^{18}O_{fc}$ depletions reported from Pliocene sapropels [*Emeis et al.*, 2000a; *Thunell et al.*, 1984]. Significantly larger $\Delta\delta^{18}O_{seawater}$ estimates result from maximum and minimum $\Delta\delta^{18}O_{fc}$ and the associated SST change (Table 4). We note a stronger depletion starting with S7 compared with older sapropels, and in most cases the depletion is largest on the Mediterranean Ridge south of Crete. In all cases except S8, $\delta^{18}O_{seawater}$ is more depleted in the eastern than in the western Mediterranean Sea (Table 4).

4.3. Geographical Patterns

[30] The modern gradient in $\delta^{18}O_{seawater}$ of surface waters is from 0.8 to 1.4‰ in the western Mediterranean, and from 1.3 to 1.7‰ in the eastern Mediterranean, i.e., around 0.5‰ [*Pierre*, 1999]. The gradient steepened by 1.1‰ during the Last Glacial Maximum and was caused by significant isotopic enrichment of $\delta^{18}O_{seawater}$ in the Levantine basin in response to decreased advection of Atlantic inflow and increased evaporation [*Rohling and de Rijk*, 1999]. Based on numerous isotope records, these authors also established eastward increasing $\delta^{18}O_{seawater}$ during the Holocene optimum and sapropel S1 time, but found that the gradient was only approximately 50% of its present-day magnitude and was caused mainly by largest relative depletion in the Levantine Sea: For the youngest sapropel S1, the glacial-interglacial difference in $\delta^{18}O_{seawater}$ was −0.8‰ in the western basin, −1‰ in the central eastern basin, and −2.2‰ in the Levantine Basin. *Rohling and de Rijk* [1999] concluded that the Mediterranean Sea continued to operate as a concentration

basin during S1 formation, but that the freshwater deficit was substantially smaller than today. In their view, reasons for the diminished freshwater deficit centered in the easternmost Mediterranean Sea may have been seasonally enhanced Nile discharge, more depleted isotopic composition of Nile discharge, or decreased evaporation rates caused by lower wind speed, higher air humidity, or reduced temperature differences between air and sea surface.

[31] To search for first-order spatial patterns in the isotopic depletion of surface seawater, we used the data in Table 4a to solve the paleotemperature equation [*Shackleton*, 1974] for $\delta^{18}O_{seawater}$. Neglecting the global ice effect (which is the same in both basins) and based on only two records (the Balearic Rise core and the record of largest depletion in the eastern basin from Table 4a), we consistently find a glacial enrichment in the eastern Mediterranean Sea (Table 4b). An exception is during MIS 6, when the enrichment was equal in both basins. During sapropel periods, the gradient was consistently reversed, and $\delta^{18}O_{seawater}$ was depleted more in the eastern basin than in the western basin (Table 4b). The data thus are consistent with either enhanced freshwater inflow, decreased evaporative loss of freshwater, or with stronger isotopic depletion of freshwater sources to the eastern Mediterranean during all sapropel periods. Unfortunately, the geographical location of the maximum depletion in our records from the eastern Mediterranean Sea are mainly ODP Site 969 or neighboring core 71 on the Mediterranean Ridge. This is tantalizing, because that area is located in the eastward surface water flow of modified Atlantic water, which has been shown to persist under glacial and sapropel conditions [*Myers et al.*, 1998], and is not close to any of the modern sources of fresh water. More indirect clues to the dominant freshwater source are not helpful either. The magnitude of the reconstructed $\Delta\delta^{18}O_{seawater}$ change has no statistically significant relationship with either the monsoon index, or the peak insolation at 65°N in summer (Table 4a). This mismatch is difficult to reconcile with exclusive or dominant freshwater sources in the Nile catchment, the size of which should depend on monsoon strength, or in the northern catchment, the size of which should be indirectly or directly related to NH insolation.

[32] However, our core from the Levantine basin is not optimally positioned to monitor Nile water outflow, because it is outside the path of Nile river that is deflected eastward by Coriolis forcing. Also, the data may be too sparse in some of the intervals preceding sapropels to bracket the full variation in $\Delta\delta^{18}O_{seawater}$. It is possible that a number of freshwater sources may have drained the South-eastern Sahara [*Pachur and Kröpelin*, 1987] and may have discharged through modern Libya. In summary, our data are consistent with an initial sudden influx of monsoon precipitation during summer, when winds are weak and mixing and dispersal of freshwater is impeded. As we discuss below, further evidence for a monsoon imprint and thus for a southern source are the strong depletions seen in all eastern records around 150 kyr and at S6 time.

4.4. Implications for the Trigger for Stratification

[33] The potential for the development of anoxia is high during transitions from cold and arid to warm and humid phases, because deep basins were filled with salty and cold deep water emplaced during the preceding glacials [*Rohling*, 1994]. Density of surface water decreased in the late glacial and post glacial due to inflow of fresh water and warming, and the density decrease was enforced by lack of deep convection so that fresher water pooled in the surface. The initial inflow of less dense water was the trigger that shut off deep convection long enough to establish a stable pycnocline. Stratification must have been stable enough so that winter density gains by cooling of the surface mixed layer were smaller than the density difference in midwater. The Old Deep Water (ODW) became anoxic rapidly, because the oxygen gained by downward eddy diffusion had been outstripped by oxygen demand of sinking detritus [*Mangini and Schlosser*, 1986]. The higher density decayed significantly less rapidly than the oxygen content of the ODW, decreasing only by salt loss to overlying water and heating from below. Added salt input from dissolution of Messinian salt in the subsurface may in part have replenish the salt lost by diffusion [*Kullenberg*, 1952; *Myers et al.*, 1998; *Rossignol-Strick*, 1987]. Lack of convection concentrated isotopically light and relatively fresher waters in the surface layer. In concert with stronger heating during insolation maxima, the density of surface waters continued to decrease and remained lower than that of ODW. Thermal inertia of the water masses caused increasing SST in surface waters even when winters were more severe under conditions of higher seasonal contrasts that accompany lower insolation in winter. The annual overturn (triggered by winter cooling of surface waters) continued to some extent and replenished nutrients in the surface water, but convection was shallower [*Myers et al.*, 1998]. Thus the density contrast between cold, salty and eventually anoxic ODW and a warming and less dense surface layer persisted over 2000–3000 years, i.e., for the duration of sapropel deposition [*Myers et al.*, 1998]. Stratification broke up when the pycnocline was increasingly eroded by increasingly deeper convection in the late stages of sapropel formation, and when the trend to decreasing density of surface water ended.

[34] The scenario of sapropel formation as a consequence of an initially strong and gradually weakening contrast in deep and surface water density properties at climatic transitions would not require a substantial decrease of surface water $\delta^{18}O_{seawater}$ and salinity. It would be a process that is to a significant extent aided by warming of surface waters: the steeper the warming trend, the longer can the density difference be maintained. But how can we reconcile the glacial sapropels S6 and S8 with this scenario?

4.5. The "Glacial" Sapropels S6 and S8

[35] The records of S6 and S8 indicate that SST were as low as 12°C during S6 and at the base of S8 (Figure 2b). The low temperature estimates for the two glacial sapropels are fully in agreement with pollen and faunal records and suggest that they formed while large ice-sheets were extant in the high latitudes [*Cita et al.*, 1977; *Rossignol-Strick and Paterne*, 1999; *Vergnaud-Grazzini et al.*, 1977]. Estimated mean annual temperatures at the northern coast of the Mediterranean have been 10°C colder than present during

Table 4a. Summary of Information on External (Global Ice Volume) and Regional Influences on the Isotopic Composition of Seawater Before and During Sapropel Formation[a]

Sapropel	Time Interval, kyr	Δ SST, °C	$\Delta\delta^{18}O$, ‰	Maximum Ice Effect,[b] ‰	T Effect, ‰	$(\Delta\delta\ ^{18}O)_{seawater,}$ ‰	Monsoon[c]	NH Insolation,[d] W m^{-2}	Δ Salinity
S1	18-7	2.5	−1.7	−0.94	−0.5	−0.3	42	497	−1
S3	91-80	1.7	−1.2	−0.34	−0.3	−0.5	46	501	−2
S4	111-100	0.6	−0.7	−0.47	−0.1	−0.1	46	500	0
S5	135-122	5.9	−2.7	−1.24	−1.2	−0.3	59	518	−1
S6	183-170	−4.6	−1.4	−0.34	0.9	−3.2	51	508	−13
S7	201-191	4.0	−1.5	−0.08	−0.8	−0.6	54	500	−3
S8	225-213	2.3	−1.1	−0.33	−0.5	−0.3	63	520	−1
S9	248-239	4.0	−1.5	−0.32	−0.8	−0.4	44	504	−2
S10	340-332	1.0	−0.3	−0.58	−0.2	0.4	53	511	2

[a]Given are median changes of SST and $\delta^{18}O$ from Table 3. Ice volume changes from cold isotope events before to of each sapropel have been estimated for the listed time intervals [*Vogelsang*, 1990]. The estimates of median and maximal SST change are from Table 3, as are changes in $\delta^{18}O_{fc}$. The Monsoon Index values [*Rossignol-Strick and Paterne*, 1999] and the June insolation curve at 65°N [*Laskar et al.*, 1993] at the onset of sapropel deposition show no correlation with $\delta^{18}O_{seawater}$. The age for the base of S1 is in calendar years.
[b]Within time interval considered; data from *Vogelsang* [1990].
[c]Index at sapropel base [*Rossignol-Strick*, 1983].
[d]From *Laskar et al.* [1993].

the last glacial maximum, with a steep gradient to permafrost conditions near 45°N [*Bigg*, 1995]. Similar temperature gradients can be assumed for glacial stages 7d (sapropel S8) and early stage 6 (sapropel S6).

[36] Sapropel S8 nevertheless conforms to the pattern proposed above in that the sapropel follows a phase with higher $\delta^{18}O_{seawater}$ and lower temperatures, which would have been the time of ODW emplacement (Figure 4a). S8 initiated near the end of the brief but intensely glacial isotopic substage 7d, coeval with the similarly very cold and arid pollen zone G in Macedonia [*Wijmstra and Smit*, 1976]. The pollen record of the northern catchment indicates mean temperature of ∼2°C for winter, ∼18°C for summer and mean monthly precipitation of ∼30 mm for winter and ∼20 mm for summer [*Wijmstra et al.*, 1990]. These conditions reflect the presence of large ice-sheets during a full glacial period to the North, creating conditions that are arid and cold. It is not likely that significant freshwater would come from that area. Modulation of the precessional cycles by eccentricity cycles generated the maximum amplitude of the precession index variation, successively the deepest insolation valley at 231 kyr and the highest insolation peak at 220 kyr. This extreme contrast caused different climatic responses at different latitudes. In the high latitudes, the deep insolation valley at 231 kyr generated the rapidly accumulated ice sheet of isotopic substage 7d, and the inertia of the ice-sheet retarded the melting phase associated with the 220kyr insolation peak. In the low latitudes, the monsoon responded without lag to the 220 kyr insolation peak [*Rossignol-Strick*, 1983, 1985]. Sapropel 8 thus started to deposit in response to the low-latitude monsoon forcing earlier than the deglaciation, so

Table 4b. $\delta^{18}O_{seawater}$ Calculated From the Paleotemperature Equation [*Shackleton*, 1974] for Each Glacial-Interglacial Transition in the Eastern and Western Mediterranean Sea[a]

Sapropel	Time Interval, kyr	ΔSST, °C	$\Delta\delta^{18}O$, ‰	Maximum Ice Effect, ‰	T Effect, ‰	$(\Delta\delta\ ^{18}O)_{seawater,}$‰	Monsoon	NH Insolation, W m^{-2}
				Minimum and Maximum Values of $\delta^{18}O_{fc}$/Eastern Mediterranean				
S1/969	18-9	6.6	−4.3	−0.73	−1.3	−2.3	42	497
S3/969	85-82	0.7	−2.7	0.10	−0.1	−2.7	46	501
S4/969	111-104	2.9	−3.3	−0.16	−0.6	−2.6	46	500
S5/967	135-126	6.7	−4.6	−1.10	−1.3	−2.2	59	518
S6/969	182-176	−2.1	−4.3	−0.05	0.4	−3.0	51	508
S7/967	201-196	3.5	−3.0	−0.06	−0.7	−2.2	54	500
S8/969	225-213	2.2	3.2	−0.09	−0.4	−0.5	63	520
S9	248-239	5.1	−1.9	−0.32	−1.0	−0.6	44	504
S10	335-334	2.0	−1.0	0.00	−0.4	−0.6	53	511
Sapropel	Time Interval, kyr	Δ SST, °C	$\Delta\delta^{18}O$, ‰	Maximum Ice Effect,[b] ‰	T Effect, ‰	$(\Delta\delta\ ^{18}O)_{seawater,}$ ‰	Difference E-W	
				Minimum and Maximum Values of $\delta^{18}O_{fc}$ Western Mediterranean				
S1	18-9	3.5	−2.6	−0.73	−0.7	−1.2	−1.1	
S3	88-81	6.6	−0.8	−0.28	−1.3	0.8	−3.5	
S4	110-103	2.0	−1.3	−0.23	−0.4	−0.7	−1.9	
S5	135-124	8.9	−3.5	−1.15	−1.8	−0.6	−1.6	
S6	182-176	−1.6	−3.1	−0.05	0.3	−2.9	−0.1	
S7	200-195	2.1	−1.5	−0.06	−0.4	−1.0	−1.2	
S8	224-218	0.8	−1.6	−0.06	−0.2	−0.8	0.3	

[a]Given are extreme values of SST and $\delta^{18}O$ from Table 3. Data on $\delta^{18}O_{fc}$ and SST are from Table 4a for maximum enrichments/depletions during each period.

that the Mediterranean region was still in its glacial mode and SST was cold.

[37] The depletion in $\delta^{18}O_{bulloides}$ is strong (Figure 3) and indicates an abrupt initial decrease in $\delta^{18}O_{seawater}$ at Site 967 that is not matched by a temperature or ice volume change of similar magnitude. The signal is thus entirely consistent with a massive influx of isotopically depleted monsoon precipitation. From that initial negative spike in the Site 967 record $\delta^{18}O$ of *G. bulloides* (and later, of *G. ruber*; Figure 3) increase toward the top against the temperature trend and suggest increasing $\delta^{18}O_{seawater}$ (and salinity). It is probably the increasing SST that sustained density stratification and isolation of ODW; enhanced inflow of humidity from the northern catchment is not likely because the pollen records of S8 suggests cold and arid conditions in the catchment [*Rossignol-Strick and Paterne*, 1999]. Input of water depleted in $\delta^{18}O$ must have been sporadic to cause the highly variable $\delta^{18}O$ record of *G. bulloides* in S8, suggesting that stratification was weaker in the case of S8 than in other cases. This is also suggested by a relatively weak depletion in residual $\delta^{18}O$ (Table 4a), whereas the difference between the eastern and the western Mediterranean basins was significant (Table 4b).

[38] Sapropel S6 remains to be explained. It has the largest depletion in $\delta^{18}O_{seawater}$, but the gradient in $\delta^{18}O_{sea\text{-}seawater}$ between the eastern and western Mediterranean Sea was small (Table 4b). This lack of a gradient may reflect three influences: In the western Mediterranean Sea, inflowing North Atlantic surface water may have been depleted in the wake of ice-sheet melting and was not yet enriched by evaporation at the location of our core. Second, elevated continental runoff caused by southward displacement of atmospheric low pressure zones may have increased precipitation in the catchment of the western Mediterranean Sea [*Nicholson and Flohn*, 1980]. Third, the eastern Mediterranean Sea was significantly more fertile prior to and during S6 than in any other sapropel period [*Schmiedl et al.*, 1998] which implies that stratification must have been weak before and after S6 [*Castradori*, 1993]. Mixing of surface and intermediate waters thus was more vigorous, and pooling of depleted waters was less effective in the eastern Mediterranean Sea.

[39] The low temperatures in the center of S6 develop against a general decrease in ice volume (solid curve in Figure 4b) and near peak insolation. They are again matched by pollen data and suggest that the northern periphery of the Mediterranean Sea was glaciated, cold and arid, an unlikely source for significant amounts of precipitation and river runoff. The truly massive depletion of at least -3‰ in the $\delta^{18}O_{seawater}$ (Table 4a) apparently occurred at the very base of S6; the increased oxygen demand caused by increased fertility must have led to the initiation of anoxia very shortly after stratification.

[40] Two sources for the isotopically depleted surface water are possible. Our preferred source is increased monsoonal rainfall in the southern catchment [*Masson et al.*, 2000]. In their climate model simulation with insolation forcing at 175 kyr and glacial boundary conditions, these authors show that the mean annual freshwater balance for the Mediterranean Sea (precipitation minus evaporation plus continental runoff) increased by 0.7 m per year, composed of a reduction in evaporation and increased outflow from the Nile river. The northern African summer precipitation was intensified by 30% and may also have been channeled into the eastern Mediterranean via Libya. Our preference for the monsoonal trigger is further based on the large isotope depletion seen around 150 kyr in the continuous records (Figure 4b). It is analogous in orbital configuration to the time around 525 kyr, when a massive odd monsoon [*Rossignol-Strick et al.*, 1998] caused an unusually timed sapropel in the eastern Mediterranean Sea. The depletion at 150 kyr marks an unusually strong monsoon that did not manage to push the deep water into anoxia. Notably, SST in the Mediterranean Sea remained low at that time (Figure 2b); they were depressed by continental glaciation in the periphery. The equatorial South Atlantic, on the other hand (a major moisture source of the African monsoon) was uncharacteristically warm during isotope stage 6 [*Schneider et al.*, 1996] and may have fuelled increased monsoon discharge into the Mediterranean Sea. It appears, however, that the surface water freshening associated with the depletion event at 150 kyr alone was not sufficient to push the eastern Mediterranean Sea into permanent stratification.

[41] The second source of freshwater during S6 may have been melting ice in the northern catchment. The temperature and isotope data are consistent with the idea that S6 must have formed as a consequence of massive meltwater discharge [*Thunell et al.*, 1983]. The isotopically light water may have originated either from the Eurasian Ice Sheet and may have entered the eastern basin from the Black Sea, or may have come from alpine glaciers. The initial warming and late-stage cooling limbs of the SST curve of S6 may be remains of the aborted regular sequence of events that lead to stratification and sapropel formation under favorable conditions of surface warming and moderate changes in surface salinity. The rapid and dramatic cooling embedded in S6 resembles short and intense climatic fluctuations known to accompany hydrological changes in the North Atlantic Ocean as a response to decaying ice sheets and freshwater discharges [*Barber et al.*, 1999; *Bond et al.*, 1992; *Broecker et al.*, 1988; *Fairbanks*, 1989] (Figure 4). However, such a meltwater event is unlikely under fully glacial conditions at 150 kyr.

5. Conclusions

[42] Sea-surface temperatures estimated from $U^{k'}_{37}$ indices and $\delta^{18}O$ of planktonic foraminiferal calcite suggest that sapropels in the late Quaternary eastern Mediterranean Sea formed in response to temperature- and salinity-induced stratification, which led to stagnation and anoxic conditions in deep waters. SST increase and the global ice effect contributed significantly to depletion of $\delta^{18}O_{fc}$ at transitions from cold to warm climatic stages, when sapropels formed. During most glacial stages preceding sapropels, surface water in the eastern Mediterranean Sea was isotopically enriched over the western basin. During most sapropel events, surface seawater in the eastern basin was more depleted. The range of local $\delta^{18}O_{seawater}$ depletion associated with the transition from glacial to sapropel conditions is between 0.5‰ and 3.0‰. Most high-resolution isotope records reveal that the depletion occurred some cm below or

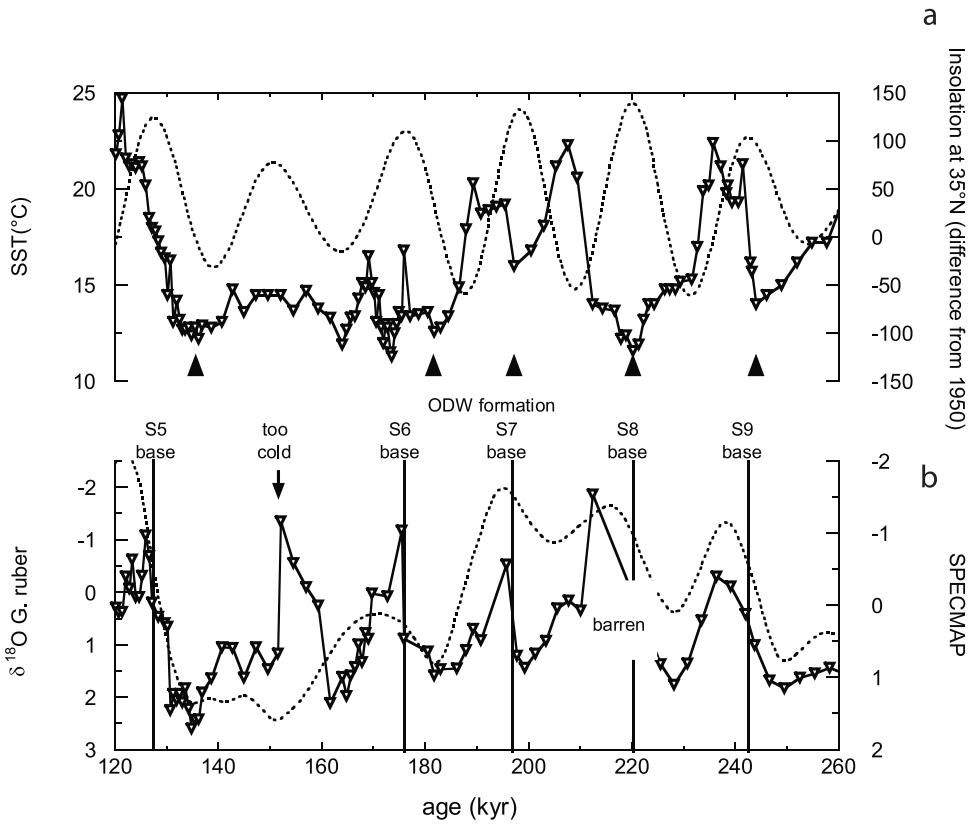

Figure 4. (a) The sea surface temperature evolution in the record of core M40-4/71 (the bases of sapropels are marked by a gray line) and the regional summer insolation curve (dashed curve; June at 35°N, deviation from 1950 value ([langleys m^{-2} d^{-1}) [*Berger*, 1978]. (b) The δ^{18}O ratios of *G. ruber* calcite and the SPECMAP curve (dashed line), a representation of ice volume changes [*Imbrie et al.*, 1984].

at the bases of sapropels, which is consistent with an initial inflow of fresh water at an early stage of enhanced insolation. Depletion is in most cases pronounced in the area south of Crete, which is not close to any present-day sources of freshwater. In our interpretation, increased capture of moisture by the southern catchment of the Mediterranean Sea from an intensified monsoonal circulation is the most likely explanation for the initial depletion. The location of strongest depletion suggests significant influx of water via fossil drainage systems in modern Libya. The initial trigger prevented convection and resulted in a pooling of isotopically depleted and less dense water at the sea surface. In addition, stratification was maintained by increasing SST during the course of the sapropel period.

[43] **Acknowledgments.** We acknowledge helpful reviews by 3 anonymous reviewers and discussions with C. Hemleben, E. Rohling and S. Weldeab. K.E. and H.S. acknowledge funding (contracts Em 37/4 and Em 37/8) by the German Research foundation and by the European Commission (ENV4-CT97-0564 TEMPUS). K.E. also acknowledges the Japanese Society for the Advancement of Science for a grant to visit to Sapporo, when the first draft was written. D.K. was funded by a NERC grant (GST/02/1229). D. Rosenberg and S. Lage performed the alkenone analyses. The Ocean Drilling Program provided the samples of Leg 160 drill sites.

References

Allen, J. R., et al., Rapid environmental changes in southern Europe during the last glacial period, *Nature*, *400*, 740–743, 1999.

Barber, D. C., et al., Forcing of the cold event of 8,200 years ago by catastrophic drainage of Laurentide lakes, *Nature*, *400*, 344–348, 1999.

Bard, E., F. Rostek, and C. Sonzogni, Interhemispheric synchrony of the last deglaciation inferred from alkenone palaeothermometry, *Nature*, *385*, 707–710, 1997.

Berger, A. L., Long-term variations of caloric insolation resulting from the earth's orbital elements, *Quat. Res.*, *9*, 139–167, 1978.

Béthoux, J.-P., Mediterranean sapropel formation, dynamic and climatic viewpoints, *Oceanol. Acta*, *16*(2), 127–133, 1993.

Béthoux, J.-P., and C. Pierre, Mediterranean functioning and sapropel formation: Respective influences of climate and hydrological changes in the Atlantic and the Mediterranean, *Mar. Geol.*, *153*, 29–39, 1999.

Bigg, G. R., Aridity of the Mediterranean Sea at the last glacial maximum: A reinterpretation of the δ^{18}O record, *Paleoceanography*, *10*, 283–290, 1995.

Bond, G., et al., Evidence for massive discharges of icebergs into the North Atlantic during the last glacial period, *Nature*, *360*, 245–249, 1992.

Brassell, S. C., G. Eglinton, I. T. Marlowe, U. Pflaumann, and M. Sarnthein, Molecular stratigraphy: A new tool for climatic assessment, *Nature*, *320*, 129–133, 1986.

Brasseur, P., J.-M. Brankart, J.-M. Beckers, and M. Rixen, Seasonal Variability of Hydrological Fields in the Mediterranean Sea, Geohydrodyn. and Environ. Res., Univ. of Liège, Liège, France, 1996.

Broecker, W. S., M. Andree, W. Wolfli, H. Oeschger, G. Bonani, J. Kennett, and D. Peteet, The chronology of the last deglaciation: Implications to the cause of the younger Dryas Event, *Paleoceanography*, *3*, 1–19, 1988.

Cacho, I., J. O. Grimalt, C. Pelejero, M. Canals, F. J. Sierro, J. A. Flores, and N. Shackleton, Dansgaard-Oeschger and Heinbrich event imprints in Alboran Sea paleotemperatures, *Paleoceanography*, *14*, 698–705, 1999a.

Cacho, I., C. Pelejero, J. O. Grimalt, A. M. Calafat, and M. Canals, C37 alkenone measurements of sea surface temperature in the Gulf of Lions (NW Mediterranean), *Org. Geochem.*, *33*, 557–566, 1999b.

Castradori, D., Calcareous nannofossils and the origin of eastern Mediterranean sapropels, *Paleoceanography*, *8*, 459–471, 1993.

Cita, M. B., C. Vergnaud-Grazzini, C. Robert, H. Chamley, N. Ciaranfi, and S. D'Onofrio, Paleoclimatic record of a long deep-sea core from the eastern Mediterranean, *Quat. Res.*, *8*, 205–235, 1977.

Comas, M. C., et al., *Proceedings of the Ocean Drilling Program, Initial Results*, vol. 161, 1023 pp., Ocean Drill. Prog., College Station, Tex., 1996.

Cramp, A., and G. O'Sullivan, Neogene sapropels in the Mediterranean: A review, *Mar. Geol.*, *153*, 11–28, 1999.

Doose, H., F. G. Prahl, and M. W. Lyle, Biomarker temperature estimates for modern and last glacial surface waters of the California Current system between 33° and 42°N, *Paleoceanography*, *12*, 615–622, 1997.

Emeis, K.-C., A. Camerlenghi, J. A. McKenzie, D. Rio, and R. Sprovieri, The occurrence and significance of Pleistocene and upper Pliocene sapropels in the Tyrrhenian Sea, *Mar. Geol.*, *100*, 155–182, 1991.

Emeis, K.-C., D. Anderson, H. Doose, D. Schulz-Bull, and D. Kroon, Sea-surface temperatures and the history of monsoon upwelling in the NW Arabian Sea during the last 500,000 yr, *Quat. Res.*, *43*, 355–361, 1995.

Emeis, K.-C., H.-M. Schulz, U. Struck, T. Sakamoto, H. Doose, H. Erlenkeuser, M. Howell, D. Kroon, and M. Paterne, Stable isotope and temperature records of sapropels from ODP Sites 964 and 967: Constraining the physical environment of sapropel formation in the Eastern Mediterranean Sea, *Proc. ODP Sci. Results*, *160*, 309–331, 1998.

Emeis, K.-C., T. Sakamoto, R. Wehausen, and H.-J. Brumsack, The sapropel record of the eastern Mediterranean Sea—Results of Ocean Drilling Program Leg 160, *Palaeogeogr. Palaeoclimatol. Palaeoecol.*, *158*, 259–280, 2000a.

Emeis, K.-C., U. Struck, H.-M. Schulz, S. Bernasconi, T. Sakamoto, and F. Martinez-Ruiz, Temperature and salinity of Mediterranean Sea surface waters over the last 16,000 years: Constraints on the physical environment of S1 sapropel formation based on stable oxygen isotopes and alkenone unsaturation ratios, *Palaeogeogr. Palaeoclimatol. Palaeoecol.*, *158*, 259–280, 2000b.

Epstein, S., H. A. Buchsbaum, H. A. Lowenstam, and H. C. Urey, Revised carbonate-water isotopic temperature scale, *Bull. Geol. Soc. Am*, *64*, 1315–1326, 1953.

Fairbanks, R. G., A 17,000-year glacio-eustatic sea level record: Influence of glacial melting rates on the Younger Dryas event and deep-ocean circulation, *Nature*, *342*, 637–642, 1989.

Fontugne, M., and S. E. Calvert, Late Pleistocene variability of the carbon isotopic composition of organic matter in the eastern Mediterranean Sea: Monitor of changes in carbon sources and atmospheric CO_2-concentrations, *Paleoceanography*, *7*, 1–20, 1992.

Fontugne, M., M. Arnold, L. Labeyrie, M. Paterne, S. E. Calvert, and J.-C. Duplessy, Paleoenvironment, sapropel chronology and Nile River discharge during the last 20,000 years as indicated by deep-sea sediment records in the Eastern Mediterranean, *Radiocarbon*, *1994*, 75–88, 1994.

Foucault, A., and D. A. Stanley, Late Quaternary paleoclimatic oscillations in East Africa recorded by heavy minerals in the Nile delta, *Nature*, *339*, 44–46, 1989.

Gong, C., and D. J. Hollander, Evidence for differential degradation of alkenones under contrasting bottom water oxygen conditions: Implication for paleotemperature reconstructions, *Geochim. Cosmochim. Acta*, *63*(3/4), 405–411, 1999.

Hilgen, F. J., Astronomical calibration of Gauss to Matuyama sapropels in the Mediterranean and implication for the Geomagnetic Polarity Time Scale, *Earth. Planet. Sci. Lett.*, *107*, 226–244, 1991.

Hoefs, M. J. L., G. J. M. Versteegh, W. I. C. Rijpstra, J. W. de Leeuw, and J. S. Sinninghe Damsté, Postdepositional oxic degradation of alkenones: Implications for the measurement of paleo sea surface temperatures, *Paleoceanography*, *13*, 42–49, 1998.

Howell, M. W., R. C. Thunell, E. di Stefano, R. Sprovieri, E. J. Tappa, and T. Sakamoto, Stable isotope chronology and paleoceanographic history of ODP Sites 963 and 964, Eastern Mediterranean Sea, *Proc. ODP Sci. Res.*, *160*, 167–180, 1998.

Imbrie, J., J. D. Hays, D. G. Martinson, A. McIntyre, A. C. Mix, J. J. Morley, N. G. Pisias, W. L. Prell, and N. J. Shackleton, The orbital theory of Pleistocene climate: Support from a revised chronology of the marine $\delta^{18}O$ record, in *Milankovitch and Climate, Part 1*, edited by A. L. Berger et al., pp. 269–305, D. Riedel, Norwell, Mass., 1984.

Jenkins, J. A., and D. F. Williams, Nile water as a cause of eastern Mediterranean sapropel formation: Evidence for and against, *Mar. Micropaleontol.*, *9*, 521–534, 1983.

Kallel, N., M. Paterne, J.-C. Duplessy, C. Vergnaud-Grazzini, C. Pujol, L. Labeyrie, M. Arnold, M. Fontugne, and C. Pierre, Enhanced rainfall in the Mediterranean region during the last sapropel event, *Oceanol. Acta*, *20*, 697–712, 1997.

Kallel, N., J.-C. Duplessy, L. Labeyrie, M. Fontugne, M. Paterne, and M. Montacer, Mediterranean pluvial periods and sapropel formation over the last 200000 years, *Palaeogeogr. Palaeoclimatol. Palaeoecol.*, *157*, 45–58, 2000.

Keller, J., W. B. F. Ryan, D. Ninkovich, and R. Altherr, Explosive volcanic activity in the Mediterranean over the last 200,000 yr as recorded in deep-sea sediments, *Geol. Soc. Am. Bull.*, *89*, 591–604, 1978.

Kidd, R. B., M. B. Cita, and W. B. F. Ryan, Stratigraphy of eastern Mediterranean sapropel sequences recovered during Leg 42A and their paleoenvironmental significance, *Init. Rep. Deep Sea Drill. Proj.*, *42*, 421–443, 1978.

Kraml, M., Laser-$^{49}Ar/^{39}Ar$-Datierungen an distalen marinen Tephren des jung-quartären mediterranen Vulkanismus (Ionisches Meer, METEOR-Fahrt 25/4), Ph.D. dissertation, Univ. of Freiburg, Freiburg, Germany, 1997.

Krom, M., Oceanography of the eastern Mediterranean Sea, *Challenger Soc.*, *5*(3), 22–28, 1995.

Krom, M., A. Michard, R. A. Cliff, and K. Strohle, Sources of sediment to the Ionian Sea and western Levantine basin of the Eastern Mediterranean during S-1 sapropel times, *Mar. Geol.*, *160*, 45–61, 1999.

Kroon, D., I. Alexander, M. Little, L. J. Lourens, A. Matthewson, A. H. F. Robertson, and T. Sakamoto, Oxygen isotope and sapropel stratigraphy in the eastern Mediterranean during the last 4 Million years (ODP Leg 160, Site 967 results), *Proc. ODP Sci. Results*, *160*, 181–189, 1998.

Kullenberg, B., On the salinity of water contained in marine sediments, *GöteborgsKungl. Vetens. Vitter. Handl. Ser. B*, *6*, 3–37, 1952.

Lane-Serff, G. F., E. J. Rohling, H. F. Bryden, and H. Charnock, Postglacial connection of the Black Sea to the Mediterranean and its relation to the timing of sapropel formation, *Paleoceanography*, *12*, 169–174, 1997.

Laskar, J., F. Joutel, and F. Boudin, Orbital, precessional, and insolation quantities for the Earth from −20 Myr to +10 Myr, *Astron. Astrophys.*, *270*, 522–533, 1993.

Lourens, L. J., A. Antonarakou, F. J. Hilgen, A. A. M. van Hoof, C. Vergnaud-Grazzini, and W. J. Zachariasse, Evaluation of the Plio-Pleistocene astronomical timescale, *Paleoceanography*, *11*, 391–413, 1996.

Madureira, L. A. S., S. A. van Krefeld, G. Eglinton, M. H. Conte, G. Ganssen, J. A. van Hinte, and J. J. Ottens, Late Quaternary high resolution biomarker and other climate proxies in a northeast Atlantic core, *Paleoceanography*, *12*, 255–269, 1997.

Malanotte-Rizzolli, P., and A. Bergamasco, The circulation of the eastern Mediterranean, Part 1, *Oceanol. Acta*, *12*, 335–351, 1989.

Mangini, A., and P. Schlosser, The formation of eastern Mediterranean sapropels, *Mar. Geol.*, *72*, 115–124, 1986.

Martinson, D. G., N. G. Pisias, J. D. Hays, J. Imbrie, T. C. Moore, and N. J. Shackleton, Age dating and the orbital theory of the ice ages: Development of a high-resolution 0–300,000 year chronostratigraphy, *Quat. Res.*, *27*, 1–30, 1987.

Masson, V., P. Braconnot, J. Jouzel, N. de Noblet, R. Cheddadi, and O. Marchal, Simulation of intense monsoons under glacial conditions, *Geophys. Res. Lett.*, *27*(12), 1747–1750, 2000.

McCoy, F. W., *Late Quaternary Sedimentation in the Eastern Mediterranean Sea*, Harvard Univ. Press, New York, 1974.

Mix, A. C., and W. F. Ruddiman, Oxygen-isotope analyses and Pleistocene ice volumes, *Quat. Res.*, *21*, 1–20, 1984.

Müller, P. J., G. Kirst, G. Ruhland, I. von Storch, and A. Rosell-Mélé, Calibration of the alkenone paleotemperature index $UK'37$ based on core tops from the eastern South Atlantic and the global ocean (60°N–60°S), *Geochim. Cosmochim. Acta*, *62*, 1757–1772, 1998.

Myers, P. G., K. Haines, and E. J. Rohling, Modeling the paleocirculation of the Mediterranean: The last glacial maximum and the Holocene with emphasis on the formation of sapropel S1, *Paleoceanography*, *13*(6), 586–606, 1998.

Nicholson, S. E., and H. Flohn, African environmental and climatic changes and the general atmospheric circulation in late Pleistocene and Holocene, *Clim. Change*, *2*, 313–348, 1980.

Olausson, E., Studies in deep-sea cores, *Rep. Swed. Deep Sea Exped. 1947–1948*, *8*, 337–391, 1961.

Pachur, H. J., and S. Kröpelin, Wadi Howar: Paleoclimatic evidence from an extinct river system in the South Eastern Sahara, *Science*, *237*, 289–300, 1987.

Passier, H. F., H.-J. Bosch, I. A. Nijenhuis, L. J. Lourens, M. E. Böttcher, A. Leenders, J. S. Sinninghe Damsté, G. J. de Lange, and J. W. de Leeuw, Sulphic Mediterranean surface waters during Pliocene sapropel formation, *Nature*, *397*, 146–149, 1999.

Paterne, M., F. Guichard, L. Labeyrie, P. Y. Gillot, and J. C. Duplessy, Tyrrhenian Sea tephrochronology of the oxygen isotope record for the past 60,000 years, *Mar. Geol.*, *72*, 259–285, 1986.

Paterne, M., N. Kallel, L. Labeyrie, M. Vautravers, J.-C. Duplessy, M. Rossignol-Strick, E. Cortijo, M. Arnold, and M. Fontugne, Hydrological relationship between the North Atlantic Ocean and the Mediterranean Sea during the past 15–75 kyr, *Paleoceanography*, *14*, 626–638, 1999.

Pierre, C., The oxygen and carbon isotope distribution in the Mediterranean water masses, *Mar. Geol.*, *153*, 41–55, 1999.

Prahl, F. G., and S. G. Wakeham, Calibration of unsaturation patterns in long-chain ketone compositions for paleotemperature assessment, *Nature*, *330*, 367–369, 1987.

Prahl, F. G., G. J. de Lange, M. Lyle, and M. A. Sparrow, Post-depositional stability of long-chain alkenones under contrasting redox conditions, *Nature*, *341*, 434–437, 1989.

Pujol, C., and C. Vergnaud-Grazzini, Distribution patterns of live planktic foraminifers as related to regional hydrography and productive systems of the Mediterranean Sea, *Mar. Micropaleontol.*, *25*, 187–217, 1995.

Roether, W., B. B. Manca, B. Klein, D. Bregant, D. Georgopoulos, V. Beitzel, V. Kovacecic, and A. Luchetta, Recent changes in eastern Mediterranean deep water, *Science*, *271*, 333–335, 1996.

Rohling, E. J., Review and new aspects concerning the formation of eastern Mediterranean sapropels, *Mar. Geol.*, *122*, 1–28, 1994.

Rohling, E. J., Environmental control on Mediterranean salinity and $\delta^{18}O$, *Paleoceanography*, *14*, 706–715, 1999.

Rohling, E. J., and G. R. Bigg, Paleosalinity and $\delta^{18}O$: A critical assessment, *J. Geophys. Res.*, *103*, 1307–1318, 1998.

Rohling, E. J., and S. de Rijk, Holocene climatic optimum and last glacial maximum in the Mediterranean: The marine oxygen isotope record, *Mar. Geol.*, *153*, 57–75, 1999.

Rohling, E. J., and W. W. C. Gieskes, Late Quaternary changes in Mediterranean intermediate water density and formation rate, *Paleoceanography*, *4*, 531–545, 1989.

Rosell-Melé, A., E. Bard, K.-C. Emeis, P. Farrimond, J. Grimalt, P. J. Müller, and R. R. Schneider, Project takes a new look at past sea surface temperatures, *Eos Trans. AGU*, *79*(33), 393–394, 1998.

Rossignol-Strick, M., African monsoons, an immediate climate response to orbital insolation, *Nature*, *304*, 46–49, 1983.

Rossignol-Strick, M., Mediterranean Quaternary sapropels, an immediate response of the African Monsoon to variation of insolation, *Palaeogeogr. Palaeoclimatol. Palaeoecol.*, *49*, 237–263, 1985.

Rossignol-Strick, M., Rainy periods and bottom water stagnation initiating brine accumulation and metal concentration, 1, The late Quaternary, *Paleoceanography*, *2*, 333–360, 1987.

Rossignol-Strick, M., and M. Paterne, A synthetic pollen record of eastern Mediterranean sapropels of the last 1 Ma: Implications for the time-scale and formation of sapropels, *Mar. Geol.*, *153*, 221–238, 1999.

Rossignol-Strick, M., W. Nesteroff, P. Olive, and C. Vergnaud-Grazzini, After the deluge: Mediterranean stagnation and sapropel formation, *Nature*, *295*, 105–110, 1982.

Rossignol-Strick, M., M. Paterne, F. C. Bassinot, K.-C. Emeis, and G. J. de Lange, An unusual mid-Pleistocene monsoon period over Africa and Asia, *Nature*, *392*, 269–272, 1998.

Rostek, F., E. Bard, L. Beaufort, C. Sonzogni, and G. Ganssen, Sea surface temperature and productivity records for the past 240 kyr in the Arabian Sea, *Deep Sea Res., Part II*, *44*(6–7), 1461–1480, 1997.

Ryan, W. B. F., W. C. Pitman III, C. O. Major, K. Shimkus, V. Moskalenko, G. A. Jones, P. Dimitrov, N. Gorür, M. Sakinc, and H. Yüce, An abrupt drowning of the Black Sea shelf, *Mar. Geol.*, *138*(1–2), 119–126, 1997.

Sakamoto, T., T. Janecek, and K.-C. Emeis, Continuous sedimentary sequences of the eastern Mediterranean Sea: Composite depth sections of ODP Leg 160, *Proc. ODP Sci. Results*, *160*, 37–59, 1998.

Schmiedl, G., C. Hemleben, J. Keller, and M. Segl, Impact of climatic changes on the benthic foraminiferal fauna in the Ionian Sea during the last 330,000 years, *Paleoceanography*, *13*, 447–458, 1998.

Schneider, R. R., P. J. Müller, and G. Ruhland, Late Quaternary surface circulation in the east equatorial South Atlantic: Evidence from alkenone sea surface temperatures, *Paleoceanography*, *10*, 197–219, 1995.

Schneider, R. R., P. J. Müller, G. M. Ruhland, G. H. Schmidt, and G. Wefer, Late Quaternary surface temperatures and productivity in the east-equatorial South Atlantic: Responses to changes in trade/monsoon wind forcing and surface water advection, in *The South Atlantic: Present and Past Circulation*, edited by G. Wefer et al., pp. 527–551, Springer-Verlag, New York, 1996.

Shackleton, N. J., Attainment of isotopic equilibrium between ocean water and the benthonic foraminifera genus *Uvigerina*: Isotopic changes in the ocean during the last glacial, *Colloq. Int. C.N.R.S*, *219*, 203–225, 1974.

Sonzogni, C., E. Bard, F. Rostek, D. Dollfus, A. Rosell-Melé, and G. Eglinton, Temperature and salinity effects on alkenone ratios measured in surface sediments from the Indian Ocean, *Quat. Res.*, *47*, 344–355, 1997.

Ströhle, K., and M. D. Krom, Evidence for the evolution of an oxygen minimum layer at the beginning of S-1 sapropel deposition in the eastern Mediterranean, *Mar. Geol.*, *140*, 231–236, 1997.

Tang, C. M., and L. D. Stott, Seasonal salinity changes during Mediterranean sapropel deposition 9000 years b.P.: Evidence from isotopic analyses of individual planktonic foraminifera, *Paleoceanography*, *8*, 473–493, 1993.

Ternois, Y., M.-A. Sicre, A. Boireau, J.-C. Marty, and J.-C. Miquel, Production patterns of alkenones in the Mediterranean Sea, *Geophys. Res. Lett.*, *23*, 3171–3174, 1996.

Ternois, Y., M.-A. Sicre, A. Boireau, M. H. Conte, and G. Eglinton, Evaluation of long-chain alkenones as paleo-temperature indicators in the Mediterranean Sea, *Deep Sea Res., Part I*, *44*, 271–286, 1997.

Thunell, R. C., and D. F. Williams, Glacial-Holocene salinity changes in the Mediterranean Sea: Hydrographic and depositional effects, *Nature*, *338*, 493–496, 1989.

Thunell, R. C., D. F. Williams, and M. B. Cita, Glacial anoxia in the eastern Mediterranean, *J. Foraminiferal Res.*, *13*(4), 283–290, 1983.

Thunell, R. C., D. A. Williams, and P. R. Belyea, Anoxic events in the Mediterranean Sea in relation to the evolution of late Neogene climates, *Mar. Geol.*, *59*, 105–134, 1984.

Troelstra, S. R., G. M. Ganssen, K. van der Borg, and A. F. M. de Jong, A late Quaternary stratigraphic framework for eastern Mediterranean sapropel S1 based on AMS 14C dates and stable oxygen isotopes, *Radiocarbon*, *33*, 15–21, 1991.

Vergnaud-Grazzini, C., ^{18}O changes in foraminifera carbonates during the last 10^5 years in the Mediterranean Sea, *Science*, *190*, 272–274, 1975.

Vergnaud-Grazzini, C., W. B. F. Ryan, and M. B. Cita, Stable isotope fractionation, climatic change and episodic stagnation in the eastern Mediterranean during the Late Quaternary, *Mar. Micropaleontol.*, *2*, 353–370, 1977.

Villanueva, J., J. O. Grimalt, E. Cortijo, L. Vidal, and L. Labeyrie, A biomarker approach to the organic matter deposited in the North Atlantic during the last climatic cycle, *Geochim. Cosmochim. Acta*, *61*(21), 4633–4646, 1998.

Vogelsang, E., Paläo-Ozeanographie des Europäischen Nordmeeres an Hand stabiler Kohlenstoff- und Sauerstoffisotope, Ph.D. dissertation, Univ. of Kiel, Kiel, Germany, 1990.

Wijmstra, T. A., and A. Smit, Palynology of the middle part (30–78 m) of the 120 deep section in Northern Greece (Macedonia), *Acta Bot. Neerl.*, *25*, 297–312, 1976.

Wijmstra, T. A., R. Young, and H. J. L. Witte, An evaluation of the climatic conditions during the late Quaternary in northern Greece by means of multivariate analysis of palynological data and comparison with recent phytosociological and climatic data, *Geol. Mijnbow*, *69*, 243–251, 1990.

Wu, P., and K. Haines, Modeling the dispersal of Levantine Intermediate Water and its role in Mediterranean deep water formation, *J. Geophys. Res.*, *101*(C3), 6591–6607, 1996.

Zhao, M., N. A. S. Beveridge, N. J. Shackleton, M. Sarnthein, and G. Eglinton, Molecular stratigraphy of cores of NW Africa: Sea surface temperature history over the last 80 ka, *Paleoceanography*, *10*, 661–676, 1995.

Ziveri, P., A. Ruten, G. J. de Lange, J. Thomson, and C. Corselli, Present-day coccolith fluxes recorded in central eastern Mediterranean sediment traps and surface sediments, *Palaeogeogr. Palaeoclimatol. Palaeoecol.*, *158*(3–4), 175–195, 2000.

K.-C. Emeis and H. Schulz, Baltic Sea Research Institute, Seestr. 15, D-18119 Warnemuende, Germany. (kay.emeis@io-warnemuende.de; hartmut.schulz@io-warnemuende.de)

H. Erlenkeuser, Leibniz-Laboratory for Radiometric Dating and Stable Isotope Research, Kiel University, Max-Eyth-Str. 11, D-24118 Kiel, Germany. (HErlenkeuser@leibniz.uni-kiel.de)

M. W. Howell, Department of Geological Sciences, University of South Carolina, Columbia, SC 29208, USA. (howell@geol.sc.edu)

S. Ishizuka, The Education Bureau of Aomori Prefecture, Seihoku Educational Office, 10 Sakaecho, Aza, Goshogawara, Aomori Prefecture, 037-0046, Japan. (satue@insoaomori.ne.jp)

D. Kroon, Faculty of Earth Sciences, Vrije Universiteit Amsterdam, De Boelelaan 1085, N-1081 HV Amsterdam, Netherlands. (kroo@geo.vu.nl)

A. Mackensen, Alfred-Wegener-Institut für Polar- und Meeresforschung, Columbusstraße, D-27568 Bremerhaven, Germany. (amackensen@AWI-Bremerhaven.de)

T. Oba, Graduate School of Environmental Earth Science, Hokkaido University, Nishi 5, Kita 10, Kitaku, Sapporo 060-0810, Japan. (oba-tad@ees.hokudai.ac.jp)

M. Rossignol-Strick, Laboratoire de Paléobiologie et Palynologie, Université Pierre et Marie Curie, 4 Place Jussieu, F-75252 Paris cedex 5, France. (mrstrick@ccr.jussieu.fr)

T. Sakamoto and I. Koizumi, Department of Earth and Planetary Sciences, Graduate School of Science, Hokkaido University, N-10 W-8, Kitaku, Sapporo 060, Japan. (tats-ron@jamstec.go.jp)

U. Struck, Institute of Paleontology and Historical Geology, University of Munich, Richard-Wagner-Strasse 10, D-80333 Munich, Germany. (u.struck@lrz.uni-muenchen.de)